Analyzing Multi-Stage Loss Curves: Plateau and Descent Mechanisms in Neural Networks

Zheng-An Chen¹, Tao Luo¹,²,* Guihong Wang¹†
¹ School of Mathematical Sciences, Shanghai Jiao Tong University
²Institute of Natural Sciences, MOE-LSC, Shanghai Jiao Tong University;
CMA-Shanghai, Shanghai Artificial Intelligence Laboratory

Abstract

The multi-stage phenomenon in the training loss curves of neural networks has been widely observed, reflecting the non-linearity and complexity inherent in the training process. In this work, we investigate the training dynamics of neural networks (NNs), with particular emphasis on the small initialization regime and identify three distinct stages observed in the loss curve during training: initial plateau stage, initial descent stage, and secondary plateau stage. Through rigorous analysis, we reveal the underlying challenges causing slow training during the plateau stages. Building on existing work, we provide a more detailed proof in the initial plateau. This is followed by a comprehensive analysis of the dynamics in the descent stage. Furthermore, we explore the mechanisms that enable the network to overcome the prolonged secondary plateau stage, supported by both experimental evidence and heuristic reasoning. Finally, to better understand the relationship between global training trends and local parameter adjustments, we employ the Wasserstein distance to capture the microscopic evolution of weight amplitude distribution.

Keywords: two-layer neural networks, multi-stage analysis, loss curve, small initialization, plateau and descent

1 Introduction

In recent years, deep learning has achieved remarkable advancements in various fields [22, 5, 17, 20]. Research on the training process plays a crucial role in understanding and applying neural networks (NNs). Unlike traditional machine learning, neural networks present a highly-dimensional and complex loss landscape, which makes optimization challenging. Researchers [16, 6, 19] have long discovered multi-stage characteristic on the loss curve. During the training process, the loss may stay at a plateau but then suddenly plunge with no apparent reason, which demonstrates the complexity and non-uniformity of training dynamics. Understanding the plateau and descent mechanisms is essential for optimizing neural network.

The choice of parameter initialization is of vital importance on both the training dynamics and characteristics of the loss curve. For large initialization, the dynamics of neural networks can be approximated by a kernel regression framework known as the neural tangent kernel (NTK) [8, 7, 1], where parameters remain close to their initialization throughout training and loss continues to uniformly decline. Situated between large and small initialization, the gradient flow (GF) of

^{*}corresponding author, luotao41@sjtu.edu.cn

[†]in alphabetic order

neural networks can be captured by nonlinear partial differential equations (PDEs) from a mean field perspective [14, 21, 18, 4], offering insights into how networks transition between different dynamical regimes. At the other end of the spectrum, small initialization induces a condensation effect, where parameters will initially aggregate along a few directions during the early stage of training [12, 25, 2, 3, 15]. Subsequently, the dynamics transition through multiple nonlinear stages. This phenomenon is particularly interesting as it reflects a more active exploration of the parameter space and will be the focus of our subsequent analysis.

Previous studies on small initialization mainly focus on the initial stage of training, revealing the condensation phenomenon for multi-layer feedforward neural networks [3] and convolutional neural networks [26]. However, these studies largely overlook the characterization of the subsequent stages in the loss curve.

In this work, we conduct a multi-stage analysis of the loss curve and identify three distinct stages in the early training process: the initial plateau stage, the initial descent stage, and the secondary plateau stage, based on their manifestations on the curve. The dynamics governing these stages are driven by different dominant mechanisms, ranging from linear to nonlinear behavior. We provide rigorous theoretical analysis of the dynamics within each stage and use macroscopic quantities to uncover the underlying causes behind both the plateau and descent stages.

2 Contribution and Related Works

2.1 Our contribution

In this paper, we consider two-layer NNs, formulated as $f_{\theta}(x) = \sum_{k=1}^{m} a_k \sigma(\mathbf{w}_k^{\top} x)$, where m is the width of the neural network and θ including a_k and \mathbf{w}_k are i.i.d. sampled from $\mathcal{N}(0, \frac{1}{m^{2\alpha}})$ and $\mathcal{N}(0, \frac{1}{m^{2\alpha}} \mathbf{I}_d)$. Without loss of generality, we consider the gradient flow and denote T_0 as the beginning of the training in this paper. We consider the range of the model in applications for supervised learning where α is greater than $\frac{1}{2}$. Empirically, we have discovered that the onset of training loss curved can be divided into three distinct stages: the initial plateau stage, the initial descent stage and the secondary plateau stage, which is shown in Fig. 1. The plateau and descent stages are quite common on the loss curve of training [6], but need a more comprehensive consideration. In this work, we aim to figure out the intrinsic dynamics of these stage and theoretically give a rigorous clarification. We will discuss these three stages separately, and encapsulate our findings in more digestible forms (Theorems 1*, 2*, 3*, and 4*) before the main results, to help the comprehension of the dynamical behavior behind the loss curve.

• Initial Plateau Stage: Under the setting of small initialization, the model frequently goes through a stage of stagnation as seen in Fig. 1(a), akin to the "warming up" period for the parameters. During this period the parameters behaves more in a linear pattern, which has been investigated in [2] and is referred to as initial condensation. We present a new proof for the behavior of neural networks during this stage, refining previous results with a more rigorous theoretical approach.

Theorem 1* (Informal statement of Theorem 1: Initial plateau stage). For $\alpha > \frac{1}{2}$, with a high probability over the choice of $\boldsymbol{\theta}$, there exists T_p such that

$$T_{\rm p} = \Omega(\log m),\tag{1}$$

and the average decay rate of initial plateau stage is given by

$$\lim_{m \to +\infty} \frac{|R(\boldsymbol{\theta}(T_{p})) - R(\boldsymbol{\theta}(T_{0}))|}{T_{p} - T_{0}} = 0.$$
 (2)

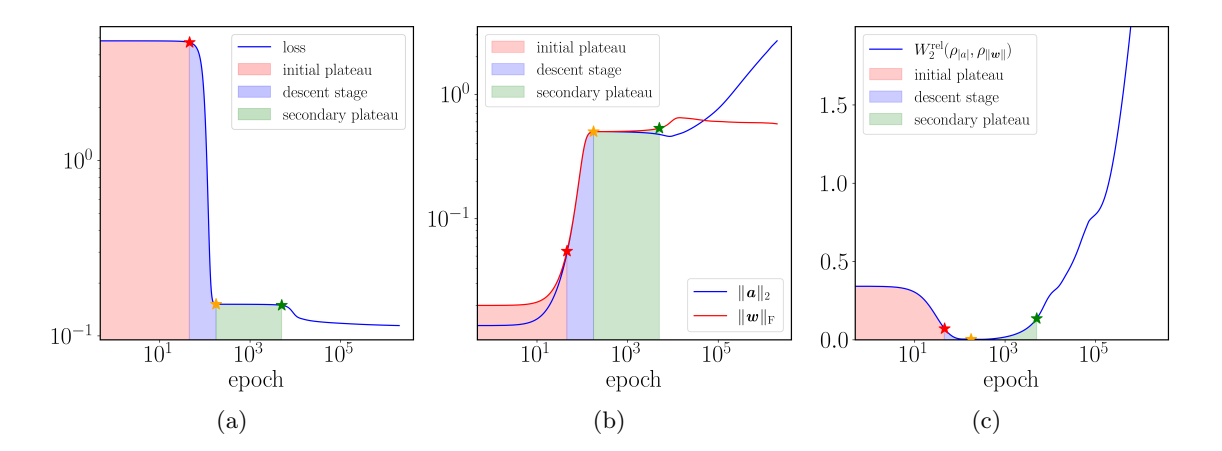


Figure 1: The behavior of training loss (panel a), norms of weights (panel b) and relative Wasserstein distance between weights (panel c) that is $W_2^{\text{rel}}(\rho_{|a|}, \rho_{||\boldsymbol{w}||}) = W_2(\rho_{|a|}, \rho_{||\boldsymbol{w}||})/||\rho_{|a|}||_2$ during training process. The red region is the initial plateau stage, the blue region is the initial descent stage, and the green region is the secondary plateau stage.

In Theorem 1*, T_p is the duration of the initial plateau stage which corresponds to the red star in Fig. 1. This theorem characterizes T_p with respect to width m and provide a characterization of the training loss remaining stationary. Specifically, the average decay rate of the loss is very small, indicating that the loss does not decrease significantly during this stage. For a more detailed statement, please refer to Theorem 1.

• Initial Descent Stage: After the initial plateau stage, we will give a theorem to offer deeper insights on the network's transition into more nonlinear behavior. This analysis emphasizes how the network's structure begins to evolve in this crucial stage. During this period the dynamics is moving towards an approximate critical point.

Theorem 2* (Informal statement of Theorem 2: Initial descent stage). For $\alpha > \frac{1}{2}$, with a high probability over the choice of $\boldsymbol{\theta}$, there exists $T_{\rm d}$ such that

$$\lim_{m \to \infty} \frac{T_{\rm d}}{\log m} = \frac{2\alpha - 1}{2},\tag{3}$$

and the ratio of average decay rate between initial descent stage and initial plateau stage is given by

$$\lim_{m \to +\infty} \frac{|R(\boldsymbol{\theta}(T_{\mathrm{d}})) - R(\boldsymbol{\theta}(T_{\mathrm{p}}))|}{|R(\boldsymbol{\theta}(T_{\mathrm{p}})) - R(\boldsymbol{\theta}(T_{0}))|} \frac{|T_{\mathrm{p}} - T_{0}|}{|T_{\mathrm{d}} - T_{\mathrm{p}}|} = +\infty.$$

$$(4)$$

In Theorem 2*, T_d refers to the endpoint of the descent stage which is the yellow star in Fig. 1 and T_p is mentioned in Theorem 1*. This theorem gives a stronger description of T_d which is solely dependent on m and α , as checked experimentally in Section 4.2.2. Moreover, the decrease in loss during the descent stage occurs at a higher rate compared to the initial plateau stage, resulting in a significant descent. This relative increase in the average decay rate of the loss indicates a more pronounced reduction during this stage. A more rigorous statement is provided in Theorem 2.

• Secondary Plateau Stage: In this stage, the dynamics is near an approximate critical point and wanders around the vicinity for a long time. Therefore, the loss curve illustrates another plateau stage.

Theorem 3* (Informal statement of Theorem 3: Secondary plateau stage). For $\alpha > \frac{1}{2}$, with a high probability over the choice of $\boldsymbol{\theta}$, there exists $T_{\rm sp}$ such that

$$\lim_{m \to +\infty} \frac{T_{\rm sp}}{\log m} = +\infty,\tag{5}$$

and the ratio of average decay rate between secondary plateau stage and initial descent stage is given by

$$\lim_{m \to +\infty} \frac{|R(\boldsymbol{\theta}(T_{\rm sp})) - R(\boldsymbol{\theta}(T_{\rm d}))|}{|R(\boldsymbol{\theta}(T_{\rm d})) - R(\boldsymbol{\theta}(T_{\rm p}))|} \frac{|T_{\rm d} - T_{\rm p}|}{|T_{\rm sp} - T_{\rm d}|} = 0.$$
 (6)

Here $T_{\rm sp}$ is the end point of the secondary plateau stage which is the green star in Fig. 1 and $T_{\rm d}$, $T_{\rm p}$ are mentioned above. This theorem illustrates both the duration of the stage and the plateau effect, emphasizing that during this period, the average decay rate of the loss is significantly lower compared to the previous stage, resulting in a slow change in loss.

Moreover, we dig into the behavior of parameters and introduce the Wasserstein distance as a novel tool to describe the microscopic evolution of weight distributions during training. Here we state an informal theorem based on results of Corollaries 1 and 4 to show that different types of weights converge to the same distribution during the training.

Theorem 4*. (Informal statement of Corollaries 1 and 4: Amplitude distribution of weights are similar) For $\alpha > \frac{1}{2}$, for any $t \in [T_p, T_d]$

$$\lim_{m \to +\infty} \frac{W_2(\rho_{|a|}, \rho_{||w||})}{W_2(\rho_{|a|})} = 0.$$
 (7)

Here $T_{\rm p}$ and $T_{\rm d}$ are mentioned above. We can see in Fig. 1(c) that the relative Wasserstein distance declines since the descent stage during which the norms of the weights are in the same level in Fig. 1(b). Moreover, using experimental data and heuristic reasoning, we explore the factors that allow the network to exit the secondary plateau and offer intuition into the mechanisms driving the network's progression beyond this stage in Section 4.3.2.

By quantifying both global trends and local changes in neural parameters behavior, our results underscore the need to understand neural network dynamics at multiple scales. These insights can offer practical implications for improving network generalization and optimization strategies. Theorems 1*, 2*, 3*, and 4* and alignment of the milestones in the subgraph of Fig. 1 implies a story theoretically and experimentally: During training under small initialization, the loss remains stationary while the parameters is moving towards in the same direction. Once they achieve a similar distribution, the loss begins to decrease until the dynamics approaches an approximate critical point and settles into a secondary plateau. As the weights strive to separate, the loss leaves the plateau and begins to decrease once more.

2.2 Related Works

Here, we discuss some related work. In fact, our nonlinear model can be viewed as a perturbation of a homogeneous linear model in its early stages. The homogeneous model has been widely applied in analyzing both the early stage and final stage dynamics of parameter behavior.

• Early stage analysis: There has been some work on early stage analysis. In matrix factorization problems, the model can be viewed as shallow or deep linear networks, though the problem remains

non-convex. [24] shows that randomly initialized gradient descent converges to a global minimum of the asymmetric low-rank factorization problem at a polynomial rate. However, this model is linear. To some extent, our work builds on these approaches by extending them to nonlinear models. Studies such as [2, 3, 11] characterize the initial stage where parameters condense or their directions converge in nonlinear models, though they do not fully capture the subsequent stages. [15] identifies different stages for classification problems with separable data. However, due to certain limitations in the data and the structure of the loss function, it does not yet fully account for the secondary plateau stage and the transition from linear to nonlinear models.

• Final stage analysis: Other notable works focus on the convergence properties of homogeneous models in the final stages of classification where researchers often start their work under the assumption of correct classification. [13] models the final state as a max-margin optimization problem and get the convergence of both the normalized margin and its smoothed version to the objective value at a KKT point. Furthermore, [9] extends the previous results and achieves directional convergence outcomes. Although the problems may seem different, as demonstrated in [10], we believe that these two categories are fundamentally related.

The rest of the paper is organized as follows: Section 3 covers preliminary work, including the introduction of notation, the problem formulation, and key insights of different stages. Section 4 outlines our theoretical framework and the main results. The appendix contains propositions that aid in the proofs, along with detailed experimental results.

3 Preliminaries

3.1 Notations

First, we introduce some notations that will be used in the rest of this paper. Let m be the width of hidden layers. Let [n] denote the set of integers from 1 to n and [k:n] be the set of integers from k to n. Denote vector L^2 norm as $\|\cdot\|_2$. For a vector \mathbf{v} , denote its k-th entry as \mathbf{v}^k . We use $O(\cdot)$ and $\Theta(\cdot)$ for the standard Big-O and Big-Theta notations. For those nontrivial notations, we can refer to the Appendix A.

3.2 Problem formulation

We consider two-layer neural networks with smooth activation function. In the whole analysis, We believe that linear network will approximate the nonlinear network well under small initialization setting until some time. The main issue is when this approximation will fail. In the process of exploring this question, we will gradually deepen our understanding of key phenomena such as condensation phenomena and the plateau phenomenon in the loss curve.

The model we now consider is

$$f_{\boldsymbol{\theta}}(\boldsymbol{x}) = \sum_{k=1}^{m} a_k \sigma(\boldsymbol{w}_k^{\top} \boldsymbol{x}),$$

with initial parameter $a_k(0) = N(0, \frac{1}{m^{2\alpha}})$ and $\boldsymbol{w}_k(0) = N(0, \frac{1}{m^{2\alpha}}\boldsymbol{I}_d)$. For simplicity, we consider the following population risk function (also known as population loss function):

$$R(\boldsymbol{\theta}) = \frac{1}{2} \int_{\mathbb{R}^d} \left(f_{\boldsymbol{\theta}}(\boldsymbol{x}) - f(\boldsymbol{x}) \right)^2 \rho(\boldsymbol{x}) \, \mathrm{d}\boldsymbol{x}.$$

Without loss of generality, we make the following assumptions to normalize our problem.

Assumption 1 (Symmetric sampling probability). Density function $\rho(\mathbf{x})$ has compact support. Moreover, $\int_{\mathbb{R}^d} x_i^2 \rho(\mathbf{x}) d\mathbf{x} = 1$ for $i \in [d]$ and $\int_{\mathbb{R}^d} x_i x_j \rho(\mathbf{x}) d\mathbf{x} = 0$ for $i \neq j$, $i, j \in [d]$.

Assumption 2 (Non-vanishing leading term). The initial condensation direction is non-degenerate. That is

 $\int_{\mathbb{R}^d} f(\boldsymbol{x}) \boldsymbol{x} \rho(\boldsymbol{x}) \, \mathrm{d}\boldsymbol{x} = (1, 0, \dots, 0)^{\top}.$

Remark 1. It should be noted that we only use the symmetry of the distribution. So it is actually a over-parameterized case and the result can be applied to situations with very few sample data where R is the empirical loss/risk and ρ is the sum of delta functions. Our result also can be extended to the networks with bias.

We assume our activation function like tanh function, which includes a class of smooth activation functions. Without loss of generality, we take the following assumption.

Assumption 3 (Tanh-like activation function). The activation function σ satisfies: $\sigma(0) = 0, \sigma^{(1)}(0) = 1, \sigma^{(2)}(0) = 0, |\sigma^{(3)}(z)| \le C_L$ for all $z \in \mathbb{R}$.

Assumptions 1, 2, and 3 are applied throughout the analysis in this paper. Based on these assumptions, we approximate gradient descent using gradient flow under the condition that the learning rate is sufficiently small. Consequently, the system dynamics can be expressed as follows (with the detailed derivation provided in the Appendix).

$$\begin{cases}
\frac{\mathrm{d}a_k}{\mathrm{d}t} = w_k^1 - \left(\sum_{l=1}^m a_l w_l^1\right) w_k^1 - \sum_{i=2}^d \left(\sum_{l=1}^m a_l w_l^i\right) w_k^i + f_k, \\
\frac{\mathrm{d}\boldsymbol{w}_k}{\mathrm{d}t} = -\int_{\mathbb{R}^d} \left(\sum_{l=1}^m a_l \left(\boldsymbol{w}_l^\top \boldsymbol{x}\right) - f(\boldsymbol{x})\right) a_k \boldsymbol{x} \rho(\boldsymbol{x}) \, \mathrm{d}\boldsymbol{x} + \boldsymbol{g}_k,
\end{cases} \tag{8}$$

where the superscript in w_k^i means the *i*-th entry. Here the higher-order term f_k and g_k are defined as follows:

$$f_{k} = \int_{\mathbb{R}^{d}} f(\boldsymbol{x}) \left(\frac{1}{3!} \sigma^{(3)}(\xi_{k}(\boldsymbol{x})) (\boldsymbol{w}_{k}^{\top} \boldsymbol{x})^{3} \right) \rho(\boldsymbol{x}) d\boldsymbol{x}$$

$$- \int_{\mathbb{R}^{d}} \left(\sum_{l=1}^{m} \frac{1}{3!} \sigma^{(3)}(\xi_{l}(\boldsymbol{x})) a_{l} (\boldsymbol{w}_{l}^{\top} \boldsymbol{x})^{3} \right) (\boldsymbol{w}_{k}^{\top} \boldsymbol{x}) \rho(\boldsymbol{x}) d\boldsymbol{x}$$

$$- \int_{\mathbb{R}^{d}} \left(\sum_{l=1}^{m} a_{l} \left(\boldsymbol{w}_{l}^{\top} \boldsymbol{x} + \frac{1}{3!} \sigma^{(3)}(\xi_{l}(\boldsymbol{x})) (\boldsymbol{w}_{l}^{\top} \boldsymbol{x})^{3} \right) \right) \left(\frac{1}{3!} \sigma^{(3)}(\xi_{k}(\boldsymbol{x})) (\boldsymbol{w}_{k}^{\top} \boldsymbol{x})^{3} \right) \rho(\boldsymbol{x}) d\boldsymbol{x}.$$

$$\boldsymbol{g}_{k} = \int_{\mathbb{R}^{d}} f(\boldsymbol{x}) a_{k} \left(\frac{1}{2!} \sigma^{(3)} (\eta_{k}(\boldsymbol{x})) \left(\boldsymbol{w}_{k}^{\top} \boldsymbol{x} \right)^{2} \right) \boldsymbol{x} \rho(\boldsymbol{x}) d\boldsymbol{x}$$

$$- \int_{\mathbb{R}^{d}} \left(\sum_{l=1}^{m} a_{l} \left(\boldsymbol{w}_{l}^{\top} \boldsymbol{x} \right) \right) a_{k} \left(\frac{1}{2!} \sigma^{(3)} (\eta_{k}(\boldsymbol{x})) \left(\boldsymbol{w}_{k}^{\top} \boldsymbol{x} \right)^{2} \right) \boldsymbol{x} \rho(\boldsymbol{x}) d\boldsymbol{x}$$

$$- \int_{\mathbb{R}^{d}} \left(\sum_{l=1}^{m} a_{l} \frac{1}{3!} \sigma^{(3)} (\xi_{l}(\boldsymbol{x})) \left(\boldsymbol{w}_{l}^{\top} \boldsymbol{x} \right)^{3} \right) a_{k} \left(1 + \frac{1}{2!} \sigma^{(3)} (\eta_{k}(\boldsymbol{x})) \left(\boldsymbol{w}_{k}^{\top} \boldsymbol{x} \right)^{2} \right) \boldsymbol{x} \rho(\boldsymbol{x}) d\boldsymbol{x}.$$

$$(9)$$

where $\xi_k(\boldsymbol{x})$ and $\eta_k(\boldsymbol{x})$ comes from Taylor's expansion. To better reveal the structure of the dynamics, we can express \boldsymbol{w}_k in its component form.

$$\begin{cases}
\frac{da_k}{dt} = w_k^1 - \left(\sum_{l=1}^m a_l w_l^1\right) w_k^1 - \sum_{i=2}^d \left(\sum_{l=1}^m a_l w_l^i\right) w_k^i + f_k, \\
\frac{dw_k^1}{dt} = a_k - \left(\sum_{l=1}^m a_l w_l^1\right) a_k + g_k^1, \\
\frac{dw_k^i}{dt} = -\left(\sum_{l=1}^m a_l w_l^i\right) a_k + g_k^i.
\end{cases} (10)$$

We will estimate the higher-orders carefully throughout this paper. To achieve this, we introduce neuron-wise L^{∞} norm called q_{max} which is defined as follows:

$$q_{\max}(t) = \max_{k \in [m], i \in [d]} \{|a_k(t)|, |w_k^i(t)|\}.$$
(11)

By direct computation, it can be shown that these terms are negligible in the stages we are concerned with, as formalized in the following lemma.

Lemma 1 (Estimate of higher order terms). The following inequalities hold for $q_{max} \leq 1$:

$$|f_k|, \|g_k\|_2 \le C_L(q_{\max}^3 + mq_{\max}^5).$$
 (12)

3.3 Separation of different stages: an intuitive discussion

According to the behavior of loss during the training process, we divide the initial and intermediate stages of training into three stages: the initial plateau stage, the initial descent stage, and the secondary plateau stage, as shown in the Fig. 1(a). These three stages constitute the primary focus of this paper.

We introduce Wasserstein distance to characterize difference between the empirical distribution of input weights and output weights. Recall the Wasserstein distance is defined as

$$W_2(\rho_1, \rho_2) = \inf_{\gamma \in \mathcal{C}(\rho_1, \rho_2)} \left(\int \|\boldsymbol{\theta}_1 - \boldsymbol{\theta}_2\|_2^2 \gamma(\mathrm{d}\boldsymbol{\theta}_1, \mathrm{d}\boldsymbol{\theta}_2) \right)^{\frac{1}{2}}, \tag{13}$$

where the infimum is taken over all couplings of ρ_1 and ρ_2 . That is γ is a joint probability distribution defined on $\mathbb{R}^m \times \mathbb{R}^m$, such that its marginal distributions are ρ_1 and ρ_2 , respectively. We consider empirical distribution $\rho_{|a|} = \frac{1}{m} \sum_{k=1}^m \delta_{|a_k|}$ and $\rho_{||\mathbf{w}||} = \frac{1}{m} \sum_{k=1}^m \delta_{||\mathbf{w}_k||}$. There is an upper bound we will use in the following discussion.

$$W_2(\rho_{|a|}, \rho_{||\boldsymbol{w}||}) \le \left(\frac{1}{m} \sum_{k=1}^m (|a_k| - ||\boldsymbol{w}_k||)^2\right)^{\frac{1}{2}}.$$
 (14)

As shown in Fig.1, during the three stages of the training loss curve, the norms of the weights and their relative Wasserstein distance change synchronously. On the one hand, the norms of \boldsymbol{w} and \boldsymbol{a} progressively approach equality at the red star in Fig.1 which is the beginning of the descent stage. On the other hand, at the end of the descent stage, that is the yellow star, both the norms of the weights seem to settle onto the same plateau and the relative Wasserstein distance vanishes to zero. In Fig.1, We aim to illustrate that the phenomenon depicted in the figure, from right to

left, can be described as an observation of the same process transitioning from the microscopic to the macroscopic scale. More specifically, we can observe that the microscopic changes often occur slightly before the macroscopic changes, which is quite natural, much like the intense molecular motion that accompanies the heating of water before any noticeable temperature increase occurs. In this paper, we will theoretically analyze the dynamical behavior of the weights during each period. Here, we outline the main ideas behind the proof.

In the initial stage, due to the very small initialization, the parameters will be approximated by the linear dynamics described below. As a result, the weight vector will be proved to condense in a specific direction starting from a randomly initialized state by error estimate between Eqs. (10) and (15). It is important to note that we have established a similar result in [2], but in this work, we employ a different technique to obtain improved estimates.

$$\begin{cases}
\frac{\mathrm{d}a_k}{\mathrm{d}t} = w_k^1, \\
\frac{\mathrm{d}w_k^1}{\mathrm{d}t} = a_k, \\
\frac{\mathrm{d}w_k^i}{\mathrm{d}t} = 0, \quad i = 2, \dots, d.
\end{cases}$$
(15)

In the initial descent stage, after considering higher order approximation, the dynamics of parameters will be governed by the following system:

$$\begin{cases}
\frac{\mathrm{d}a_k}{\mathrm{d}t} = w_k^1 - \left(\sum_{l=1}^m a_l w_l^1\right) w_k^1, \\
\frac{\mathrm{d}w_k^1}{\mathrm{d}t} = a_k - \left(\sum_{l=1}^m a_l w_l^1\right) a_k, \\
\frac{\mathrm{d}w_k^i}{\mathrm{d}t} = 0, \quad i = 2, \dots, d.
\end{cases}$$
(16)

It is important to note that we will consider the dynamics described by Eq. (10), the properties of which can be determined through Eq. (16), rather than conducting an error estimate. In this part, we introduce

$$K = \sum_{k=1}^{m} a_k w_k^1,$$

$$K' = \sum_{k=1}^{m} \left(a_k^2 + (w_k^1)^2 \right).$$
(17)

Considering the dynamics of K, we find that it approximately follows

$$\frac{\mathrm{d}K}{\mathrm{d}t} = 2K(1-K). \tag{18}$$

Fortunately, Eq. (18) admits an explicit solution:

$$K(t) = \frac{C(t_0)e^{2(t-t_0)}}{1 + C(t_0)e^{2(t-t_0)}},$$
(19)

where $C(t_0) = \frac{K(t_0)}{1 - K(t_0)}$ when $K(t_0) \neq 1$. It is clear that the dynamics in Eq. (18) will rapidly converge to a "critical point", corresponding to the condition K = 1.

In the secondary plateau stage, since the dynamics has converged to a critical point, the entire dynamics enter a prolonged stagnation stage to explore new directions. This is reflected on the loss curve as an extended plateau. At this point, the effective dynamics will be dominated by the following dynamics. This is because we start from a "critical point" corresponding to the condition K=1 and then the leading term will vanish since

$$w_k^1 - \left(\sum_{l=1}^m a_l w_l^1\right) w_k^1 = (1 - K) w_k^1 \approx 0,$$

$$a_k - \left(\sum_{l=1}^m a_l w_l^1\right) a_k = (1 - K) a_k \approx 0.$$
(20)

Thus, the evolution of the parameters at this point can be approximated by the following equation:

$$\begin{cases}
\frac{\mathrm{d}a_k}{\mathrm{d}t} = -\sum_{i=2}^d \left(\sum_{l=1}^m a_l w_l^i\right) w_k^i + f_k, \\
\frac{\mathrm{d}w_k^1}{\mathrm{d}t} = g_k^1, \\
\frac{\mathrm{d}w_k^i}{\mathrm{d}t} = -\left(\sum_{l=1}^m a_l w_l^i\right) a_k + g_k^i, \quad i = 2, \dots, d.
\end{cases} \tag{21}$$

Throughout the three stages of the proof, we will find the following lemma particularly useful, as it separates w_k^1 from the other directions w_k^i and decouples the complicated dynamics (10) into simple form in three stages. This result stems from an observation of the dynamics and the loss landscape during the stages we consider under small initialization.

Lemma 2 (Growth lemma). Let $T_{\text{test}} = \left\{ t \geq 0 \mid q_{\text{max}} \leq \frac{1}{m^{\beta}} (\log m)^{\gamma} \right\}$ where $\beta, \gamma \in \mathbb{R}_+$ such that $\frac{1}{m^{\beta}} (\log m)^{\gamma} \leq 1$. We have for $i = 2, \ldots, d, \ t_0 \leq t \leq T_{\text{test}}$

$$\left(\sum_{k=1}^{m} \left(w_k^i(t)\right)^2\right)^{\frac{1}{2}} \le \left(\sum_{k=1}^{m} \left(w_k^i(t_0)\right)^2\right)^{\frac{1}{2}} + C \max\left\{\frac{(\log m)^{3\gamma}}{m^{3\beta - \frac{1}{2}}}, \frac{(\log m)^{5\gamma}}{m^{5\beta - \frac{3}{2}}}\right\} (t - t_0). \tag{22}$$

Remark 2. The moment T_{test} serves as an intuitive conjecture regarding the neuron-wise L^{∞} norm q_{max} at various stages.

Proof. Through direct computation, we find that the leading term is negative, which provides an upper bound,

$$\frac{\mathrm{d}\left(\sum_{k=1}^{m}(w_{k}^{i})^{2}\right)}{\mathrm{d}t} = 2\sum_{k=1}^{m}w_{k}^{i}\left(-a_{k}\left(\sum_{k=1}^{m}a_{k}w_{k}^{i}\right) + g_{k}^{i}\right)$$

$$\leq 2\left(\sum_{k=1}^{m}(w_{k}^{i})^{2}\right)^{\frac{1}{2}}\left(\sum_{k=1}^{m}(g_{k}^{i})^{2}\right)^{\frac{1}{2}}.$$

By lemma 1 and the definition of T_{test} , we have

$$\left(\sum_{k=1}^{m} (g_k^i)^2\right)^{\frac{1}{2}} \le C\sqrt{m} \max\left\{q_{\max}^3, mq_{\max}^5\right\}$$

$$\le C \max\left\{\frac{(\log m)^{3\gamma}}{m^{3\beta - \frac{1}{2}}}, \frac{(\log m)^{5\gamma}}{m^{5\beta - \frac{3}{2}}}\right\}.$$

As a result,

$$\left(\sum_{k=1}^{m} (w_k^i(t))^2\right)^{\frac{1}{2}} \le \left(\sum_{k=1}^{m} (w_k^i(t_0))^2\right)^{\frac{1}{2}} + C \max\left\{\frac{(\log m)^{3\gamma}}{m^{3\beta - \frac{1}{2}}}, \frac{(\log m)^{5\gamma}}{m^{5\beta - \frac{3}{2}}}\right\} (t - t_0).$$

4 Main Results

4.1 Initial plateau stage

In this section, We will prove that linearized flow (15) will approximate dynamics (10) well in the initial stage. This result is rephrased from [2], but the proof approach is not entirely the same, and it yields more refined results. The improvement primarily stems from Lemma 2.

Let \tilde{a}_k and \tilde{w}_k^i denote the solutions of Eq. (15) with the same initial conditions as those in Eq. (10). It has analytical solution as follows,

$$\tilde{a}_{k}(t) = \frac{1}{2}(a_{k}(0) + w_{k}^{1}(0))e^{t} + \frac{1}{2}(a_{k}(0) - w_{k}^{1}(0))e^{-t},
\tilde{w}_{k}^{i}(t) = \frac{1}{2}(a_{k}(0) + w_{k}^{1}(0))e^{t} - \frac{1}{2}(a_{k}(0) - w_{k}^{1}(0))e^{-t},
\tilde{w}_{k}^{i}(t) = w_{k}^{i}(0), \quad i = 2, \dots, d.$$
(23)

Similarly, we define \tilde{q}_{max} as follows.

$$\tilde{q}_{\max} = \max_{k \in [m], i \in [d]} \{ |\tilde{a}_k(t)|, |\tilde{w}_k^i(t)| \}.$$
(24)

We denote the difference between Eq. (10) and the linearized flow (15) by

$$r_{\max}(t) = \max_{k \in [m]} \left\{ |a_k(t) - \tilde{a}_k(t)| + |w_k^1(t) - \tilde{w}_k^1(t)| \right\}. \tag{25}$$

We use the following test time T_1 to characterize the effect time of linearization.

$$T_1 = \inf \left\{ t \ge 0 \mid q_{\max} \ge \frac{1}{m^{\alpha_1}} \log m, r_{\max} \ge \frac{1}{m^{\gamma_1}} (\log m)^3 \right\},$$
 (26)

where q_{max} defined as Eq. (11) and $\frac{1}{2} < \alpha_1 < \gamma_1$. Taking hyperparameters based on Tab. 1, the main theorem can be stated as follows.

Theorem 1 (Initial plateau stage). Let $(\alpha_1, \gamma_1) = (\frac{1}{2}\alpha + \frac{1}{4}, \frac{3}{2}\alpha - \frac{1}{4})$, and $T_p = \frac{2\alpha - 1}{4}\log m$ for $\frac{1}{2} < \alpha \leq \frac{3}{2}$, while $(\alpha_1, \gamma_1) = (1, 2)$ and $T_p = (\alpha - 1)\log m$ for $\alpha > \frac{3}{2}$. Given $\delta \in (0, 1)$, for sufficiently large m, with probability at least $1 - \delta$ over the choice of $\boldsymbol{\theta}$, the following holds:

(i). Neuron-wise estimate is maintained during the initial plateau stage:

$$T_{\rm p} \le T_1. \tag{27}$$

Furthermore, for i = 2, ..., d, we have

$$\max_{k \in m, i \in [2:d]} \left\{ |w_k^i(T_p)| \right\} \lesssim \max \left\{ \frac{1}{m^\alpha} \log m, \frac{1}{m^3} (\log m)^6 \right\}. \tag{28}$$

(ii). The loss function exhibits negligible variation during the initial plateau stage:

$$\frac{|R(\boldsymbol{\theta}(T_{\mathrm{p}})) - R(\boldsymbol{\theta}(0))|}{T_{\mathrm{p}}} \lesssim \frac{1}{m^{2\alpha_1 - 1} \log m}.$$
 (29)

Remark 3. In Theorem 1, we work in a probabilistic setting, i.e., with probability $1-\delta$ the results hold, which will recur frequently in the subsequent conclusions. This is because we adopt random initialization, making the worst-case hard to avoid. However, for sufficiently large m, δ can be sufficiently small, we can see this in Lemma 3.

Remark 4. In Tab. 1, we present the values of α_1, γ_1 and T_p for different α . Here, α_1 governs the leading order behavior of q_{\max} , while γ_1 dictates the leading order of r_{\max} . Note that the division of the interval $(\frac{1}{2}, +\infty)$ into two subintervals is purely for the convenience of the subsequent proofs and does not indicate any intrinsic distinction between the two cases.

Table 1: Hyperparameters in Theorem 1

	α_1	γ_1	$T_{ m p}$
$\frac{\frac{1}{2} < \alpha \le \frac{3}{2}}{\frac{3}{2} < \alpha < \infty}$	$\frac{\frac{1}{2}\alpha + \frac{1}{4}}{1}$	$\frac{3}{2}\alpha - \frac{1}{4}$	$\frac{\frac{2\alpha-1}{4}\log m}{(\alpha-1)\log m}$

Remark 5. It should be noted that the existence of $\log m$ term is due the gaussian initialization. This initialization method produced a relative factor of the order $\log m$, which hinders us from obtaining further results through particle estimation. Fortunately, if we turn to fine estimation, we can obtain further results.

Before we make any further, we estimate $\sum_{k=1}^{m} (w_k^i)^2$ for $i=2,\ldots,d$ by Lemma 2. This term represents weights in non-condensed directions.

Proposition 1 (Estimate of weights in non-condensed directions at initial plateau stage). Let α_1, γ_1 be defined as in Theorem 1. Given $\delta \in (0,1)$, for sufficiently large m, with probability at least $1-\delta$ over the choice of $\boldsymbol{\theta}$, for $0 \le t \le \min\{T_p, T_1\}$ and $i = 2, \ldots, d$, we have

$$\left(\sum_{k=1}^{m} (w_k^i)^2\right)^{\frac{1}{2}} \le C \max\left\{\frac{1}{m^{\frac{2\alpha-1}{2}}}, \frac{(\log m)^5}{m^{\frac{5}{2}}}\right\}. \tag{30}$$

Proof. We just prove the result for $\frac{1}{2} < \alpha \le \frac{3}{2}$ and another case is similar. By growth Lemma 2 and Proposition 8,

$$\left(\sum_{k=1}^{m} (w_k^i(t))^2\right)^{\frac{1}{2}} \le \left(\sum_{k=1}^{m} (w_k^i(0))^2\right)^{\frac{1}{2}} + C \max\left\{\frac{(\log m)^3}{m^{3\alpha_1 - \frac{1}{2}}}, \frac{(\log m)^5}{m^{5\alpha_1 - \frac{3}{2}}}\right\} t$$

$$\le \frac{C}{m^{\frac{2\alpha - 1}{2}}} + C \frac{1}{m^{\frac{3}{2}\alpha + \frac{1}{4}}} (\log m)^4.$$

Since $\frac{1}{2} < \alpha \le \frac{3}{2}$, $C \frac{1}{m^{\frac{3}{2}\alpha + \frac{1}{4}}} (\log m)^4 \le \frac{1}{m^{\frac{2\alpha - 1}{2}}}$, the inequality (30) holds.

Remark 6. By comparing Eqs. (35) and (30), we observe that Proposition 1 effectively demonstrates that each w_k^i shares an equal portion of $(\sum_{k=1}^m (w_k^i)^2)$, with each w_k^i scaled by a factor of approximately $\frac{1}{\sqrt{m}}$. In other words, Theorem 1 derives an L^{∞} bound from an L^2 control.

Now we turn to the proof of Theorem 1.

Proof of Theorem 1. The proof of the theorem can be divided into two parts. We first conduct with standard error estimate by gronwall inequality and then prove by contradiction to get neuron-wise control at initial plateau stage.

(i). We measure the deviation between the linearized flow (15) and the dynamics in Eq. (10). As noted, the linearized flow (15) closely approximates dynamics (10) in the initial stage, rendering the remaining terms in Eq. (10) higher-order errors. Thus, we define F_k and G_k^i as follows

$$F_k = -\sum_{i=1}^{d} w_k^i \left(\sum_{l=1}^{m} a_l w_l^i \right) + f_k,$$

$$G_k^i = -a_k \left(\sum_{l=1}^{m} a_l w_l^i \right) + g_k^i.$$

By definitions of F_k and G_k^i , the following inequalities hold

$$|a_k(t) - \tilde{a}_k(t)| \le \int_0^t |\boldsymbol{w}_k^1 - \tilde{\boldsymbol{w}}_k^1| \, \mathrm{d}s + \int_0^t |F_k| \, \mathrm{d}s,$$
$$|\boldsymbol{w}_k^1(t) - \tilde{\boldsymbol{w}}_k^1(t)| \le \int_0^t |a_k - \tilde{a}_k| \, \mathrm{d}s + \int_0^t |G_k^1| \, \mathrm{d}s.$$

Due to $\alpha_1 > \frac{1}{2}$, it is clear that $|F_k| \leq Cmq_{\max}^3$ and $|G_k^i| \leq Cmq_{\max}^3$. Recalling the definition of r_{\max} , it follows that r_{\max} satisfies the following inequality

$$r_{\max}(t) \le \int_0^t r_{\max}(s) ds + \int_0^t Cmq_{\max}^3(s) ds.$$

Using analytical solution given in Eq. (23) and initialization estimate from Eq. (74), we obtain the following for $t \leq T_1$

$$\begin{split} r_{\text{max}} & \leq \int_0^t r_{\text{max}} \mathrm{d}s + \int_0^t Cm \frac{1}{m^{\alpha_1}} \log m q_{\text{max}}^2 \mathrm{d}s \\ & \leq \int_0^t r_{\text{max}} \mathrm{d}s + \int_0^t Cm \frac{1}{m^{\alpha_1}} \log m \left(\tilde{q}_{\text{max}}^2 + r_{\text{max}}^2 \right) \mathrm{d}s \\ & \leq \left(1 + \frac{Cm \log m}{m^{\alpha_1 + \gamma_1}} \right) \int_0^t r_{\text{max}} \mathrm{d}s + \int_0^t Cm \frac{1}{m^{\alpha_1}} \log m \left(\frac{1}{m^{\alpha}} \sqrt{2 \log \frac{2md}{\delta}} e^t \right)^2 \mathrm{d}s, \end{split}$$

where the first inequality follows from the definition of T_1 , and the third inequality is derived from the explicit solution (23). Moreover, $\frac{Cm\log m}{m^{\alpha_1+\gamma_1}} \leq 1$ for $m \geq C^{\frac{2}{2\alpha-1}}$. As a result,

$$r_{\text{max}} \le 2 \int_0^t r_{\text{max}} ds + \int_0^t Cm \frac{1}{m^{\alpha_1}} \frac{1}{m^{2\alpha}} (\log m)^2 e^{2t} ds.$$

By the Gronwall inequality, we have

$$r_{\text{max}} \le C m^{1-\alpha_1 - 2\alpha} (\log m)^2 e^{2t}. \tag{31}$$

(ii). Without loss of generality, we will provide a detailed proof for $\frac{1}{2} < \alpha \le \frac{3}{2}$, as the argument for the other case is analogous. We claim that $T_{\rm p} = \frac{2\alpha - 1}{4} \log m \le T_1$. That is, the following inequality holds for $0 < t \le T_{\rm p}$.

$$q_{\max}(t) \le \frac{1}{m^{\frac{1}{2}\alpha + \frac{1}{4}}} \log m,$$

$$r_{\max}(t) \le \frac{1}{m^{\frac{3}{2}\alpha - \frac{1}{4}}} (\log m)^{3}.$$
(32)

Now we prove by contradiction. If the assertion does not hold, then $T_1 < \frac{2\alpha - 1}{4} \log m$. Since

$$r_{\max}(T_1) \le C m^{1-\alpha_1 - 2\alpha} (\log m)^2 e^{2T_1}$$

 $< \frac{1}{m^{\alpha_1 + \alpha - \frac{1}{2}}} (\log m)^3.$

Since $\gamma_1 = \alpha_1 + \alpha - \frac{1}{2}$, we have

$$r_{\text{max}} < \frac{1}{m^{\gamma_1}} (\log m)^3. \tag{33}$$

From the solution to the linear system (23), it follows that

$$\max_{k \in [m]} \{a_k, w_k^1\} \leq \max_{k \in [m]} \{\tilde{a_k}, \tilde{w}_k^1\} + r_{\max}
\leq \frac{1}{m^{\alpha}} m^{\frac{2\alpha - 1}{4}} \sqrt{2 \log \frac{2md}{\delta}} + \frac{1}{m^{\alpha_1 + \alpha - \frac{1}{2}}} (\log m)^3
< \frac{1}{m^{\frac{1}{4} + \frac{1}{2}\alpha}} \log m.$$
(34)

Since $\alpha_1 = \frac{1}{2}\alpha + \frac{1}{4}$ and for w_k^i where $i \in [2:d]$ and $k \in [m]$, we apply Lemmas 1, 2 to obtain

$$\begin{aligned} \left| w_k^i(t) \right| &\leq \left| w_k^i(0) \right| + \int_0^t |a_k| \left(\sum_{l=1}^m |a_l| |w_l^i| \right) \mathrm{d}s + \int_0^t |g_k^i| \mathrm{d}s. \\ &\leq \left| w_k^i(0) \right| + \int_0^t |a_k| \left(\sum_{l=1}^m a_l^2 \right)^{\frac{1}{2}} \left(\sum_{l=1}^m (w_l^i)^2 \right)^{\frac{1}{2}} \mathrm{d}s + C (\log m)^4 \frac{1}{m^{\frac{3}{2}\alpha + \frac{3}{4}}} \\ &\leq \frac{1}{m^{\alpha}} \sqrt{2 \log \frac{2md}{\delta}} + C \frac{1}{m^{\frac{2\alpha - 1}{2}}} \log m \frac{1}{m^{\frac{1}{2}\alpha + \frac{1}{4}}} \frac{1}{m^{\frac{1}{2}\alpha - \frac{1}{4}}} \\ &< \frac{1}{m^{\alpha}} \log m, \end{aligned} \tag{35}$$

when m is sufficiently large. This is just Eq. (28) in Theorem 1. Consequently, from Eqs. (33), (34), and (35), we have

$$q_{\max}(T_1) < \frac{1}{m^{\alpha_1}} \log m,$$

 $r_{\max}(T_1) < \frac{1}{m^{\gamma_1}} (\log m)^3.$

This contradicts the definition of T_1 , thereby proving our claim.

Combined with some estimates on the initialization, we give the following fine estimate which will be used in following sections.

Proposition 2 (Fine estimate at the initial plateau stage). Let α_1, γ_1 , and T_p be as defined above. For $\delta \in (0,1)$ and sufficiently large m, with probability at least $1-\delta$ over the choice of $\boldsymbol{\theta}$, we obtain the following asymptotic equality at $t = T_p$:

$$\sum_{k=1}^{m} a_k w_k^1, \sum_{k=1}^{m} a_k^2 + (w_k^1)^2 = \Theta(\frac{1}{m^{2\alpha_1 - 1}}).$$
(36)

Moreover,

$$\frac{\sum_{k=1}^{m} a_k w_k^1}{\sum_{k=1}^{m} a_k^2 + (w_k^1)^2} = \frac{1}{2} + \varepsilon_1, \tag{37}$$

where $\varepsilon_1 = O(\frac{1}{m^{2\alpha_1-1}}(\log m)^4)$.

Proof. We prove the $\frac{1}{2} < \alpha \le \frac{3}{2}$ case, noting that the argument for the other case is analogous. Based on the analytical solution (23), it follows that

$$\sum_{k=1}^{m} a_k w_k^1 = \sum_{k=1}^{m} \tilde{a}_k \tilde{w}_k^1 + \sum_{k=1}^{m} a_k w_k^1 - \sum_{k=1}^{m} \tilde{a}_k \tilde{w}_k^1$$

$$= \sum_{k=1}^{m} \frac{1}{4} e^{2t} \left(a_k(0) + w_k^1(0) \right)^2 - \frac{1}{4} e^{-2t} \left(a_k(0) - w_k^1(0) \right)^2$$

$$+ \sum_{k=1}^{m} a_k (w_k^1 - \tilde{w}_k^1) + \sum_{k=1}^{m} \tilde{w}_k^1 (a_k - \tilde{a}_k).$$

According to Proposition 8, which gives the initialization estimate, when $T_p = \frac{2\alpha-1}{4} \log m$, the following inequalities hold at t = 0

$$\frac{1}{8} \frac{1}{m^{\frac{2\alpha-1}{2}}} \le \sum_{k=1}^{m} \frac{1}{4} e^{2t} \left(a_k(0) + w_k^1(0) \right)^2 \le \frac{3}{8} \frac{1}{m^{\frac{2\alpha-1}{2}}},$$

$$\frac{1}{8} \frac{1}{m^{\frac{3(2\alpha-1)}{2}}} \le \sum_{k=1}^{m} \frac{1}{4} e^{-2t} \left(a_k(0) - w_k^1(0) \right)^2 \le \frac{3}{8} \frac{1}{m^{\frac{3(2\alpha-1)}{2}}}.$$

Thanks to Theorem 1, we have

$$\left| \sum_{k=1}^{m} a_k (w_k^1 - \tilde{w}_k^1) \right| \le m q_{\max} r_{\max} \le \frac{1}{m^{2\alpha - 1}} (\log m)^4$$

because $q_{\max}(t) \leq \frac{1}{m^{\frac{1}{2}\alpha + \frac{1}{4}}} \log m$ and $r_{\max}(t) \leq \frac{1}{m^{\frac{3}{2}\alpha - \frac{1}{4}}} (\log m)^3$. As a result, we have $\sum_{k=1}^m a_k w_k^1 = \Theta(\frac{1}{m^{\frac{2\alpha - 1}{2}}}) = \Theta(\frac{1}{m^{2\alpha_1 - 1}})$.

Combining neuron-wise estimate and fine estimate at the initial plateau stage, we finish the proof of second part of Theorem 1 by direct computation as follows.

Proof. Using Taylor expansion, we will determine that

$$R(\boldsymbol{\theta}) = \frac{1}{2} \int f^{2}(\boldsymbol{x}) \rho(\boldsymbol{x}) d\boldsymbol{x} + \frac{1}{2} \sum_{i=1}^{d} \left(\sum_{k=1}^{m} a_{k} w_{k}^{i} \right)^{2} - \sum_{k=1}^{m} a_{k} w_{k}^{1} + \tilde{R},$$
(38)

where

$$\tilde{R} = \int_{\mathbb{R}^d} \left(\sum_{k=1}^m a_k \boldsymbol{w}_k^{\top} \boldsymbol{x} \right) \left(\frac{1}{3!} \sum_{k=1}^m \sigma^{(3)}(\xi_k(\boldsymbol{x})) a_k (\boldsymbol{w}_k^{\top} \boldsymbol{x})^3 \right) \rho(\boldsymbol{x}) \, d\boldsymbol{x}
+ \frac{1}{2} \int_{\mathbb{R}^d} \left(\frac{1}{3!} \sum_{k=1}^m \sigma^{(3)}(\xi_k(\boldsymbol{x})) a_k (\boldsymbol{w}_k^{\top} \boldsymbol{x})^3 \right)^2 \rho(\boldsymbol{x}) \, d\boldsymbol{x}
- \int_{\mathbb{R}^d} \left(\frac{1}{3!} \sum_{k=1}^m \sigma^{(3)}(\xi_k(\boldsymbol{x})) a_k (\boldsymbol{w}_k^{\top} \boldsymbol{x})^3 \right) f(\boldsymbol{x}) \, d\boldsymbol{x},$$
(39)

Through direct computation, the following inequality is valid when $0 \le K \le 2$ and $mq_{\text{max}} \le 1$:

$$\tilde{R} \le C m q_{\text{max}}^4. \tag{40}$$

We will then find that

$$|R(\boldsymbol{\theta}(T_{p})) - R(\boldsymbol{\theta}(0))| \leq C |K(T_{fp,\alpha}) - K(0)| + \sum_{i=2}^{d} \left(\sum_{k=1}^{m} (w_{k}^{i}(T_{fp,\alpha}))^{2} + (w_{k}^{i}(0))^{2} \right)$$

$$+ \left| \tilde{R}(T_{fp,\alpha}) - \tilde{R}(0) \right|$$

$$\leq C \frac{1}{m^{2\alpha_{1}-1}} + C \max \left\{ \frac{1}{m^{2\alpha-1}}, \frac{(\log m)^{5}}{m^{5}} \right\} + Cm \frac{(\log m)^{4}}{m^{4\alpha_{1}}}$$

$$\leq C \frac{1}{m^{2\alpha_{1}-1}},$$

$$(41)$$

since $\alpha_1 > \frac{1}{2}$ and m is sufficiently large. By combining above inequality with the definition of T_p , we finish the proof.

As a direct consequence of Theorem 1 and Proposition 2, we derive a characterization of the Wasserstein distance and the phenomenon of initial condensation. The proof is omitted for brevity.

Corollary 1 (Amplitude distribution of weights are similar at initial plateau). Let α_1, γ_1 , and T_p be as defined previously. For $\delta \in (0,1)$, with probability at least $1-\delta$ over the choice of $\boldsymbol{\theta}$, an upper bound for the relative Wasserstein distance at $t=T_p$ is given by:

$$0 \le \frac{W_2(\rho_{|a|}, \rho_{||\boldsymbol{w}||})}{W_2(\rho_{|a|})} \le C \frac{1}{m^{\gamma_1 - \alpha_1}} (\log m)^3 + C \max\left\{\frac{1}{m^{\alpha - \alpha_1}}, \frac{(\log m)^5}{m^{3 - \alpha_1}}\right\}.$$
(42)

Corollary 2 (Condensation at initial plateau (Initial condensation)). Let α_1, γ_1 , and T_p be as defined previously. For $\delta \in (0,1)$, with probability at least $1-\delta$ over the choice of $\boldsymbol{\theta}$, the following inequality holds at $t=T_p$:

$$\frac{\sum_{k=1}^{m} \|\boldsymbol{w}\|_{2}^{2}}{\sum_{k=1}^{m} (w_{k}^{1})^{2}} \ge 1 - C \max \left\{ \frac{1}{m^{2\alpha - 2\alpha_{1}}}, \frac{(\log m)^{10}}{m^{6 - 2\alpha_{1}}} \right\}.$$

$$(43)$$

Since $\alpha_1 < \min\{\gamma_1, \alpha, 3\}$, we deduce from inequality (43) that initial condensation occurs at $t = T_p$, as w_k^i , for $i \in [2, d]$, remains in a lazy state. Furthermore, the distributions of |a| and ||w|| converge to being identical for sufficiently large m, as indicated by (42).

4.2 Descent stage

4.2.1 Descent time

For the sake of brevity and readability, we will also focus on $\frac{1}{2} < \alpha \le \frac{3}{2}$ in this section, as the proof and results for $\alpha > \frac{3}{2}$ are analogous. Just as we discussed above, We want to that dynamics will converge to a critical point corresponding with K = 1 intuitively. Recall the definitions of K and K' are

$$K = \sum_{k=1}^{m} a_k w_k^1,$$

$$K' = \sum_{k=1}^{m} \left(a_k^2 + (w_k^1)^2 \right).$$

For given small $\beta > 0$, we define $T_{\rm d}$ to characterize the time for the descent stage,

$$T_{\rm d} = \inf \{ T_{\rm p} \le t \mid K \le 0, K' \le 0, 1 - K \le \beta \}.$$
 (44)

The main theorem of this section can be stated as follows.

Theorem 2 (Descent stage). For $\delta \in (0,1)$ and sufficiently large m, with probability at least $1-\delta$ over the choice of θ , for $\alpha > \frac{1}{2}$ and any given small $\beta, \delta' > 0$, the following holds:

(i). The asymptotic behavior of T_d is characterized by:

$$\frac{2\alpha - 1}{2 + \delta'} \le \frac{T_{\rm d}}{\log m} \le \frac{2\alpha - 1}{2 - \delta'} \tag{45}$$

(ii). The relative change in loss between the initial and descent stages differs significantly. Specifically, we have:

$$\frac{|R(\boldsymbol{\theta}(T_{\rm d})) - R(\boldsymbol{\theta}(T_{\rm p}))|}{|R(\boldsymbol{\theta}(T_{\rm p})) - R(\boldsymbol{\theta}(0))|} \cdot \frac{|T_{\rm p} - T_{\rm 0}|}{|T_{\rm d} - T_{\rm p}|} \ge Cm^{2\alpha_1 - 1}.$$
(46)

(iii). Furthermore, neuron-wise control holds at $t = T_d$:

$$q_{\max}(T_{\mathrm{d}}) \leq \frac{1}{m^{\frac{1}{2} - (2\alpha - 1)\delta'}},$$

$$\max_{k \in m, i \in [2:d]} \left| w_k^i(T_{\mathrm{d}}) \right| \leq \frac{1}{m^{\alpha - 2(2\alpha - 1)\delta'}}.$$

$$(47)$$

Remark 7. Theorem 2 actually shows that two-layer neural network with different scales of parameters will converge to a "critical point" at fixed time after normalization.

To prove above result, we need some prior knowledge to control weights in non-condensed directions. We define

$$T_2 = \inf\{t \mid q_{\text{max}} \ge \frac{1}{m^{\frac{1}{2} - \alpha_2}}\},$$
 (48)

where $\alpha_2 = (2\alpha - 1)\delta'$. For sufficiently large m, we can choose δ' to be arbitrarily small. Consequently, we expect a critical bound for q_{max} , as the term involving δ' approaches its limiting behavior, imposing a sharp constraint on the growth of q_{max} .

Similar to Proposition 1, we control $\sum_{k=1}^{m} (w_k^i)^2$ for $i=2,\ldots,d$ by Lemma 2.

Proposition 3 (Estimate of weights in non-condensed directions at descent stage). For $\delta \in (0,1)$ and sufficiently large m, with probability at least $1-\delta$ over the choice of $\boldsymbol{\theta}$, for $T_{\rm p} \leq t \leq \min\{T_{\rm d}, T_2, \frac{2\alpha-1}{2-\delta'}\log m\}$ and $i=2,\ldots,d$, $\sum_{k=1}^m (w_k^i)^2$ will be controlled by following inequality.

$$\left(\sum_{k=1}^{m} (w_k^i)^2\right)^{\frac{1}{2}} \le C \max\left\{\frac{1}{m^{\frac{2\alpha-1}{2}}}, \frac{\log m}{m^{1-5\alpha_2}}\right\}. \tag{49}$$

Proof. By growth Lemma 2,

$$\left(\sum_{k=1}^{m} \left(w_k^i(t)\right)^2\right)^{\frac{1}{2}} \le \left(\sum_{k=1}^{m} \left(w_k^i(T_{\mathbf{p}})\right)^2\right)^{\frac{1}{2}} + C \max\left\{\frac{1}{m^{3(\frac{1}{2}-\alpha_2)-\frac{1}{2}}}, \frac{1}{m^{5(\frac{1}{2}-\alpha_2)-\frac{3}{2}}}\right\} (t-T_{\mathbf{p}}).$$

By Proposition 1 and the chosen of small δ'

$$\left(\sum_{k=1}^{m} \left(w_k^i(t)\right)^2\right)^{\frac{1}{2}} \le C \max\left\{\frac{1}{m^{\frac{2\alpha-1}{2}}}, \frac{(\log m)^5}{m^{\frac{5}{2}}}\right\} + C \frac{1}{m^{1-5\alpha_2}}(t-T_p).$$

As a result, for $t \leq \min\{T_d, T_2, \frac{2\alpha - 1}{2 - \delta'} \log m\}$, we have

$$\left(\sum_{k=1}^{m} (w_k^i)^2\right)^{\frac{1}{2}} \le C \max\left\{\frac{1}{m^{\frac{2\alpha-1}{2}}}, \frac{\log m}{m^{1-5\alpha_2}}\right\}.$$

Based on the estimate of weights in non-condensed directions above, we obtain the following monotonicity proposition. Based on this proposition, we will estimate the rate between K and K' easily.

Proposition 4 (Monotonicity of K and K'). For $T_p \leq t \leq \min\{T_d, T_2, \frac{2\alpha - 1}{2 - \delta'} \log m\}$, K and K' increase monotonically.

Proof. We first examine the dynamics of K. According to the definition of K, we have

$$\frac{dK}{dt} = \sum_{k=1}^{m} \left(\frac{da_k}{dt} w_k^1 + a_k \frac{dw_k^1}{dt} \right)
= \sum_{k=1}^{m} \left(w_k^1 - \left(\sum_{l=1}^{m} a_l w_l^1 \right) w_k^1 - \sum_{i=2}^{d} \left(\sum_{l=1}^{m} a_l w_l^i \right) w_k^i + f_k \right) w_k^1
+ \sum_{k=1}^{m} \left(a_k - \left(\sum_{l=1}^{m} a_l w_l^1 \right) a_k + g_k^1 \right) a_k.$$

Recalling the definition of K', we obtain

$$\frac{\mathrm{d}K}{\mathrm{d}t} = K'(1-K) - \sum_{i=2}^{d} \left(\sum_{k=1}^{m} a_k w_k^i \right) \left(\sum_{k=1}^{m} w_k^1 w_k^i \right) + \sum_{k=1}^{m} w_k^1 f_k + \sum_{k=1}^{m} a_k g_k^1.$$

According to the Cauchy-Schwartz inequality, it is evident that

$$\left| \left(\sum_{k=1}^{m} a_k w_k^i \right) \left(\sum_{k=1}^{m} w_k^1 w_k^i \right) \right| \le K' \left(\sum_{k=1}^{m} (w_k^i)^2 \right) \\ \left| \sum_{k=1}^{m} w_k^1 f_k \right| + \left| \sum_{k=1}^{m} a_k g_k^1 \right| \le \sqrt{K'} \left(\sum_{k=1}^{m} f_k^2 \right)^{\frac{1}{2}}$$

Utilizing Proposition 3 and estimate of weights in non-condensed directions given in Eq. (12), we conclude

$$\left| \left(\sum_{k=1}^{m} a_k w_k^i \right) \left(\sum_{k=1}^{m} w_k^1 w_k^i \right) \right| \le CK' \max \left\{ \frac{1}{m^{2\alpha - 1}}, \frac{(\log m)^2}{m^{2 - 10\alpha_2}} \right\}$$
$$\left| \sum_{k=1}^{m} w_k^1 f_k \right| + \left| \sum_{k=1}^{m} a_k g_k^1 \right| \le \sqrt{K'} \frac{1}{m^{1 - 5\alpha_2}}.$$

By setting $\varepsilon_2 = \Theta(\max\left\{\frac{1}{m^{\frac{1}{4}}}, \frac{1}{m^{\frac{2\alpha-1}{2}}}\right\})$, the following inequalities are satisfied at T_p :

$$\sqrt{K'} \frac{1}{m^{1-5\alpha_2}} \le \varepsilon_2 K' \beta$$

$$\max \left\{ \frac{1}{m^{2\alpha-1}}, \frac{(\log m)^2}{m^{2-10\alpha_2}} \right\} \le \varepsilon_2 \beta.$$
(50)

By the way, in Theorem 1, the reason we select different T_i for different α is due to the technical requirement that the above inequality holds. That's why there is no essential difference for two cases. As a result, K will be monotonically increasing for at least a certain period of time. And we have

$$(1 - 2\varepsilon_2)K'(1 - K) \le \frac{\mathrm{d}K}{\mathrm{d}t} \le (1 + 2\varepsilon_2)K'(1 - K). \tag{51}$$

Next, we investigate the dynamics of K'. When Eq. (50) is satisfied, it follows that

$$\frac{dK'}{dt} = 4K(1 - K) - 2\sum_{i=2}^{d} \left(\sum_{k=1}^{m} a_k w_k^i\right)^2 + \sum_{k=1}^{m} a_k f_k + \sum_{k=1}^{m} w_k^1 g_k
\ge 4K(1 - K) - 2\varepsilon_2 K'(1 - K)
\ge (1 - K) \left\{ 4K(T_p) - 2\varepsilon_2 K'(T_p) + \int_{t_0}^{t} (4 - C\varepsilon_2) K'(1 - K) ds \right\}.$$

As a consequence, K' will remain monotonically increasing for at least a certain duration, implying that Eq. (50) will hold until $\min\{T_{\rm d}, T_2, \frac{2\alpha-1}{2-\delta'}\log m\}$, owing to the monotonicity of K'.

Now we want to show $\frac{K}{K'} \approx \frac{1}{2}$ until $\min\{T_{\rm d}, T_2, \frac{2\alpha - 1}{2 - \delta'} \log m\}$ and then get a control of K. The main technique we use is the conservation law. First, we have the following proposition.

Proposition 5 (Approximate conservation law). For $T_p \leq t \leq \min\{T_d, T_2, \frac{2\alpha - 1}{2 - \delta'} \log m\}$, we have:

$$\left| 4K \frac{\mathrm{d}K}{\mathrm{d}t} - K' \frac{\mathrm{d}K'}{\mathrm{d}t} \right| \le C\varepsilon_2(K')^2. \tag{52}$$

Proof. Analogous to the proof of Proposition 4, we derive

$$K\frac{dK}{dt} = KK'(1 - K) - K\sum_{i=2}^{d} \left(\sum_{k=1}^{m} a_k w_k^i\right) \left(\sum_{k=1}^{m} w_k^1 w_k^i\right) - K\left(\sum_{k=1}^{m} w_k^1 f_k + \sum_{k=1}^{m} a_k g_k\right),$$

$$K'\frac{dK'}{dt} = 4KK'(1 - K) - 2K'\sum_{i=2}^{d} \left(\sum_{k=1}^{m} a_k w_k^i\right)^2 - K'\left(\sum_{k=1}^{m} a_k f_k + \sum_{k=1}^{m} w_k^1 g_k\right).$$

Hence, it is derived that

$$4K\frac{dK}{dt} - K'\frac{dK'}{dt} = -4K\sum_{i=2}^{d} \left(\sum_{k=1}^{m} a_k w_k^i\right) \left(\sum_{k=1}^{m} w_k^1 w_k^i\right) + 2K'\sum_{i=2}^{d} \left(\sum_{k=1}^{m} a_k w_k^i\right)^2 - 4K\left(\sum_{k=1}^{m} w_k^1 f_k + \sum_{k=1}^{m} a_k g_k\right) + K'\left(\sum_{k=1}^{m} a_k f_k + \sum_{k=1}^{m} w_k^1 g_k\right).$$

By the Cauchy-Schwartz inequality, if follows that

$$\left| 4K \frac{\mathrm{d}K}{\mathrm{d}t} - K' \frac{\mathrm{d}K'}{\mathrm{d}t} \right| \le C(K')^2 \left(\sum_{i=2}^d \sum_{k=1}^m (w_k^i)^2 \right) + C(K')^{\frac{3}{2}} \sum_{k=1}^m \left(f_k^2 + (g_k^1)^2 \right)^{\frac{1}{2}} \\ \le C\varepsilon_2(K')^2.$$

Proposition 6 (Approximate equality condition). For $\delta \in (0,1)$ and sufficiently large m, with probability at least $1 - \delta$ over the choice of $\boldsymbol{\theta}$, for $T_p \leq t \leq \min\{T_d, T_2, \frac{2\alpha - 1}{2 - \delta'} \log m\}$, we have

$$\frac{K}{K'} = \frac{1}{2} + \varepsilon_3,\tag{53}$$

where $\varepsilon_3 = O \max\{\varepsilon_1, \varepsilon_2 \frac{2\alpha - 1}{2} \log m\}$. Similarly,

$$\frac{\sum_{k=1}^{m} a_k^2}{\sum_{k=1}^{m} (w_k^1)^2} = 1 + \varepsilon_3. \tag{54}$$

Proof. According to direct computation, we derive that

$$\begin{split} \frac{K}{K'} &= \sqrt{\frac{K^2(T_{\rm p}) + K^2(t) - K^2(T_{\rm p})}{K'^2(T_{\rm p}) + K'^2(t) - K'^2(T_{\rm p})}} \\ &= \sqrt{\frac{(\frac{1}{2} + \varepsilon_1)^2 K'^2(T_{\rm p}) + \frac{1}{4}(K'^2(t) - K'^2(T_{\rm p})) + \int_{T_i}^t K \frac{\mathrm{d}K}{\mathrm{d}s} - \frac{1}{4}K' \frac{\mathrm{d}K'}{\mathrm{d}s} \mathrm{d}s}{K'^2(T_{\rm p}) + K'^2(t) - K'^2(T_{\rm p})}} \\ &= \sqrt{\frac{1}{4} + (\varepsilon_1 + \varepsilon_1^2) \frac{K'^2(T_{\rm p})}{K'^2(t)} + \frac{\int_{T_i}^t K \frac{\mathrm{d}K}{\mathrm{d}s} - \frac{1}{4}K' \frac{\mathrm{d}K'}{\mathrm{d}s} \mathrm{d}s}{K'^2(t)}}. \end{split}}$$

Thanks to Propositions 4 and 5, the first equation is obtained through direct computation. When $\frac{1}{2} \leq \frac{\sum_{k=1}^{m} a_k^2}{\sum_{k=1}^{m} (w_k^1)^2} \leq 2$, K' will satisfy

$$\frac{1}{C} \sum_{k=1}^{m} (w_k^1)^2 \le K' \le C \sum_{k=1}^{m} (w_k^1)^2.$$

Then the second equation follows from above inequality and similar proof of first equality. \Box

We now proceed with the proof of the first part of Theorem 2.

Proof of Theorem 2 (Part 1). This part of the proof can be divided into two steps. First, we claim that $\min\{T_{\rm d}, T_2\} \leq \frac{2\alpha - 1}{2 - \delta'} \log m$. After that we prove $T_{\rm d} \leq T_2$. The other side of the inequality (45) is similar.

(i). From Eq. (18), it follows that for $T_p \le t \le \min\{T_d, T_2, \frac{2\alpha - 1}{2 - \delta'} \log m\}$, the inequality is satisfied

$$(1 - 2\varepsilon_2)K'(1 - K) \le \frac{\mathrm{d}K}{\mathrm{d}t} \le (1 + 2\varepsilon_2)K'(1 - K).$$

According to Proposition 6, it can be derived that

$$(2 - \varepsilon_4)K(1 - K) \le \frac{\mathrm{d}K}{\mathrm{d}t} \le (2 + \varepsilon_4)K(1 - K),$$

where $\varepsilon_4 = \min\{\varepsilon_2, \varepsilon_3\}.$

As a result, when $T_p \le t \le \min\{T_d, T_2, \frac{2\alpha - 1}{2 - \delta'} \log m\}$, the following inequality holds:

$$\frac{Ce^{(2-\varepsilon_4)(t-T_p)}}{1+Ce^{(2-\varepsilon_4)(t-T_p)}} \le K \le \frac{Ce^{(2+\varepsilon_4)(t-T_p)}}{1+Ce^{(2+\varepsilon_4)(t-T_p)}},$$

where $C = \Theta(\frac{1}{m^{\frac{2\alpha-1}{2}}})$ according to Proposition 2. It is claimed that $\min\{T_{\rm d}, T_2\} \leq \frac{2\alpha-1}{2-\delta'}\log m$. If this is not the case, it follows that

$$\begin{split} K &\geq \frac{C \mathrm{e}^{(2-\varepsilon_4)(t-T_\mathrm{p})}}{1+C \mathrm{e}^{(2-\varepsilon_4)(t-T_\mathrm{p})}} \\ &\geq \frac{\frac{C}{m^{\frac{2\alpha-1}{2}}} \mathrm{e}^{(2-\varepsilon_4)\frac{2\alpha-1}{4}(1+\frac{2\delta'}{2-\delta'})\log m}}{1+\frac{C}{m^{\frac{2\alpha-1}{2}}} \mathrm{e}^{(2-\varepsilon_4)\frac{2\alpha-1}{4}(1+\frac{2\delta'}{2-\delta'})\log m}} \\ &\geq 1-\frac{C}{m^{\frac{2\alpha-1}{4}}(\delta'-2\varepsilon_4)}. \end{split}$$

If m is sufficiently large, it leads to a contradiction since $\frac{C}{m^{\frac{2\alpha-1}{4}(\delta'-2\varepsilon_4)}} < \beta$.

(ii). Next, we assert that $T_{\rm d} \leq \frac{2\alpha-1}{2-\delta'}\log m$. Since it has been established that $\min\{T_{\rm d},T_2\} \leq \frac{2\alpha-1}{2-\delta'}\log m$, if $T_{\rm d} \leq T_2$, the proof is complete. Conversely, we proceed by contradiction. In this scenario, we have, $T_2 < T_{\rm d} \leq \frac{2\alpha-1}{2-\delta'}\log m$.

First, for w_k^i where $i \in [2:d]$ and $k \in [m]$, we have

$$\begin{aligned}
|w_{k}^{i}(T_{2})| &\leq |w_{k}^{i}(T_{p})| + \int_{T_{p}}^{T_{2}} |a_{k}| \left(\sum_{l=1}^{m} |a_{l}| |w_{l}^{i}| \right) ds + \int_{T_{p}}^{T_{2}} |g_{k}^{i}| ds \\
&\leq |w_{k}^{i}(T_{p})| + \int_{T_{p}}^{T_{2}} |a_{k}| \left(\sum_{l=1}^{m} a_{l}^{2} \right)^{\frac{1}{2}} \left(\sum_{l=1}^{m} (w_{l}^{i})^{2} \right)^{\frac{1}{2}} ds + \int_{T_{p}}^{T_{2}} |g_{k}^{i}| ds \\
&\leq \frac{1}{m^{\alpha}} \log m + C \max \left\{ \frac{1}{m^{\frac{2\alpha-1}{2}}}, \frac{\log m}{m^{1-5\alpha_{2}}} \right\} \log m \frac{1}{m^{\frac{1}{2}-\alpha_{2}}} + C \frac{1}{m^{\frac{3}{2}-5\alpha_{2}}} \\
&\leq C \left(\frac{\log m}{m^{\alpha}} + \frac{\log m}{m^{\alpha-\alpha_{2}}} + \frac{(\log m)^{2}}{m^{\frac{3}{2}-6\alpha_{2}}} \right).
\end{aligned} (55)$$

Thus, when $t \leq T_2$, we have the following for sufficiently large m:

$$\max_{k \in [m], i \in [2:d]} |w_k^i| \le C \frac{\log m}{m^{\alpha - \alpha_2}} < \frac{1}{m^{\frac{1}{2} - \alpha_2}},\tag{56}$$

which means q_{max} can only be chosen from a_k, w_k^1 at time T_2 . In particular, we get

$$\max_{k \in [m], i \in [2:d]} |w_k^i| \le \frac{1}{m^{\alpha - 2\alpha_2}}.$$

Therefore, we only need to consider a_k and w_k^1 . We will demonstrate that for $T_p \leq t \leq T_2$,

$$\frac{\mathrm{d}a_k}{\mathrm{d}t} = w_k^1 - \left(\sum_{l=1}^m a_l w_l^1\right) w_k^1 - \sum_{i=2}^d \left(\sum_{l=1}^m a_l w_l^i\right) w_k^i + f_k,
\frac{\mathrm{d}w_k^1}{\mathrm{d}t} = a_k - \left(\sum_{l=1}^m a_l w_l^1\right) a_k + g_k^1.$$

Then, for $T_p \leq t \leq T_2$, parameters a_k and w_k^1 satisfy the following inequalities:

$$|a_{k}(t)| \leq |a_{k}(T_{p})| + \int_{T_{p}}^{t} |w_{k}^{1}| ds + \int_{T_{p}}^{t} C \max \left\{ \frac{1}{m^{\frac{2\alpha-1}{2}}}, \frac{\log m}{m^{1-5\alpha_{2}}} \right\} \frac{1}{m^{\alpha-2\alpha_{2}}} + \frac{1}{m^{\frac{3}{2}-5\alpha_{2}}} ds,$$

$$|w_{k}^{1}(t)| \leq |w_{k}^{1}(T_{p})| + \int_{T_{p}}^{t} |a_{k}| ds + \int_{T_{p}}^{t} \frac{1}{m^{\frac{3}{2}-5\alpha_{2}}} ds.$$

$$(57)$$

Let $v(t) = |a_k(t)| + |w_k^1(t)|$. For $T_p \le t \le T_2$, we have the following:

$$v(t) \le C \left(\frac{\log m}{m^{\frac{1}{2}\alpha + \frac{1}{4}}} + \frac{\log m}{m^{2\alpha - \frac{1}{2} - 2\alpha_2}} + \frac{(\log m)^2}{m^{1 + \alpha - 7\alpha_2}} + \frac{\log m}{m^{\frac{3}{2} - 5\alpha_2}} \right) + \int_{T_{\mathbf{p}}}^t v(s) \mathrm{d}s.$$

As a result, we will determine at $t = T_2$ using the Gronwall inequality that

$$v(T_{2}) \leq e^{(T_{2}-T_{p})} C \left(\frac{\log m}{m^{\frac{1}{2}\alpha+\frac{1}{4}}} + \frac{\log m}{m^{2\alpha-\frac{1}{2}-2\alpha_{2}}} + \frac{(\log m)^{2}}{m^{1+\alpha-7\alpha_{2}}} + \frac{\log m}{m^{\frac{3}{2}-5\alpha_{2}}} \right)$$

$$\leq e^{(\frac{2\alpha-1}{2-\delta'}\log m - T_{p})} C \left(\frac{\log m}{m^{\frac{1}{2}\alpha+\frac{1}{4}}} + \frac{\log m}{m^{2\alpha-\frac{1}{2}-2\alpha_{2}}} + \frac{(\log m)^{2}}{m^{1+\alpha-7\alpha_{2}}} + \frac{\log m}{m^{\frac{3}{2}-5\alpha_{2}}} \right)$$

$$\leq m^{\frac{2\alpha-1}{4}} m^{(2\alpha-1)\frac{\delta'}{2(2-\delta')}} C \left(\frac{\log m}{m^{\frac{1}{2}\alpha+\frac{1}{4}}} + \frac{\log m}{m^{2\alpha-\frac{1}{2}-2\alpha_{2}}} + \frac{(\log m)^{2}}{m^{1+\alpha-7\alpha_{2}}} + \frac{\log m}{m^{\frac{3}{2}-5\alpha_{2}}} \right)$$

$$\leq C \frac{\log m}{m^{\frac{1}{2}-(2\alpha-1)\frac{\delta'}{2(2-\delta')}}}.$$

Since we take α_2 to be $(2\alpha - 1)\delta'$, we can choose m sufficiently large such that $q_{\max}(T_2) < \frac{1}{m^{\frac{1}{2} - \alpha_2}}$, which leads to a contradiction.

(iii). $T_{\rm d} \geq \frac{2\alpha-1}{2+\delta'}\log m$ is similar based on $T_{\rm d} \leq T_2 \leq \frac{2\alpha-1}{2-\delta'}\log m$ and the dynamics of K.

We prove the second part of Theorem 2 by direct computation.

Proof of Theorem 2 (Part 2). Based on the control of $\sum_{k=1}^{m} (w_k^i)^2$ and the definition of T_d , we find that

$$|R(\boldsymbol{\theta}(T_{d})) - R(\boldsymbol{\theta}(T_{p}))| \ge \left| \frac{1}{2} K^{2}(T_{d}) - K(T_{d}) \right| - \sum_{i=2}^{d} \left(\sum_{k=1}^{m} (w_{k}^{i}(T_{d}))^{2} + (w_{k}^{i}(T_{fp,\alpha}))^{2} \right) - \left| \tilde{R}(T_{fp,\alpha}) - \tilde{R}(0) \right|$$

$$\ge \frac{1}{2} (1 - \beta) - C \max \left\{ \frac{1}{m^{2\alpha - 1}}, \frac{(\log m)^{2}}{m^{2 - 10\alpha_{2}}} \right\} - Cm \frac{1}{m^{2 - 4\alpha_{2}}}$$

$$\ge \frac{1}{4}.$$
(58)

Combining Eqs. (41) and (58), we finish the proof.

As we have repeatedly mentioned, during the descent stage, the neural network converges to a point near a critical point. However, due to the presence of higher-order terms, the network does not truly converge to a strict critical point. Instead, the definition of a critical point needs to be appropriately relaxed. Based on this, we provide a definition of a relative critical point.

Based on above definition, we find that neural network will converge to a β -relative critical point at T_d .

Corollary 3 (β -relative critical point convergence). For $\delta \in (0,1)$ and sufficiently large m, with probability at least $1-\delta$ over the choice of $\boldsymbol{\theta}$, the dynamics (10) converge to a β -relative critical point at $t=T_d$, that is

$$\|\nabla R(\boldsymbol{\theta})\|_{\infty} \le \beta \|\boldsymbol{\theta}\|_{\infty}. \tag{59}$$

On the other hand, at $t = T_{fp,\alpha}$, we have

$$\|\nabla R(\boldsymbol{\theta})\|_{\infty} \ge \left(1 - \frac{C}{m^{2\alpha_1}}\right) \|\boldsymbol{\theta}\|_{\infty} \tag{60}$$

Proof. The proof of both inequalities is based on direct computation and Theorems 1,2. \Box

The following offers a broad interpretation of the Wasserstein distance.

Corollary 4 (Amplitude distribution of weights are similar at descent stage). For $\delta \in (0,1)$ and sufficiently large m, with probability at least $1-\delta$ over the choice of $\boldsymbol{\theta}$, the distribution $\rho_{|\boldsymbol{a}|}$ and $\rho_{||\boldsymbol{w}||}$ are similar at T_d . That is at $t=T_d$,

$$0 \le \frac{W_2(\rho_{|a|}, \rho_{||\boldsymbol{w}||})}{W_2(\rho_{|a|})} \le \frac{1}{m^{\alpha - \frac{1}{2}}} + C \max\left\{\frac{1}{m^{\frac{2\alpha - 1}{2}}}, \frac{\log m}{m^{1 - 5\alpha_2}}\right\}.$$
(61)

Remark 8. Corollaries 2, 4 together imply that the distributions $\rho_{|a|}$ and $\rho_{||w||}$ will remain approximately similar for an extended period.

Proof. By Theorem 1, at T_p

$$r_{\max} \le \frac{(\log m)^{\beta_2}}{m^{\gamma_1}}.$$

By direct computation, we get

$$|a_k(t) - w_k^1(t)| \le |a_k(T_p) - w_k^1(T_p)| + \int_{T_p}^t |a_k(s) - w_k^1(s)| \, \mathrm{d}s$$
$$+ \int_{T_p}^t C \max\left\{ \frac{1}{m^{\frac{2\alpha - 1}{2}}}, \frac{\log m}{m^{1 - 5\alpha_2}} \right\} \frac{1}{m^{\alpha - 2\alpha_2}} + \frac{1}{m^{\frac{3}{2} - 5\alpha_2}} \, \mathrm{d}s.$$

By gronwall inequality, we have

$$r_{\max}(T_{\mathbf{d}}) \le C e^{T_{\mathbf{d}} - T_{\mathbf{p}}} \max \left\{ \frac{(\log m)^{\beta_2}}{m^{\gamma_1}}, \frac{\log m}{m^{2\alpha - \frac{1}{2} - 2\alpha_2}}, \frac{\log m}{m^{1 + \alpha - 7\alpha_2}}, \frac{\log m}{m^{\frac{3}{2} - 5\alpha_2}} \right\}$$

$$\le C \max \left\{ \frac{(\log m)^{\beta_2}}{m^{\alpha - \alpha_2}}, \frac{\log m}{m^{\frac{3}{2}\alpha - \frac{1}{4} - 3\alpha_2}} \right\}.$$

Since α_2 can be sufficiently small when m is large, we find that

$$r_{\max}(T_{\rm d}) \le \frac{1}{m^{\frac{1}{2}\alpha + \frac{1}{4}}},$$

which means

$$\sum_{k=1}^{m} (|a_k| - |w_k^1|)^2 \le \sum_{k=1}^{m} (a_k - w_k^1)^2 \le \frac{1}{m^{\alpha - \frac{1}{2}}}.$$
 (62)

The results follows from above inequality since $\alpha > \frac{1}{2}$ and $\sum_{k=1}^{m} a_k^2 = \Theta(1)$.

4.2.2 Experiment

In this subsection, we perform experimental analyses to investigate the relationship between descent time $T_{\rm d}$ with different hyperparameters. The descent time is defined as the endpoint of the initial descent stage observed in the loss curve. After $T_{\rm d}$, the loss enters the secondary plateau stage. In Theorem 2, we have a result for $T_{\rm d}$ with respect to the initial standard deviation α and the network width m, recall the relation (3) as below

$$\lim_{m \to \infty} \frac{T_{\rm d}}{\log m} = \frac{2\alpha - 1}{2}.$$

We conduct several experiments for different α and m, identify the descent time and plot the results in Fig. 2. It can be confirmed from Fig. 2(a) that $T_{\rm d}$ indeed has a linear relationship with α for sufficient large m. Similarly, in Fig. 2(b), we can see that $T_{\rm d}$ is linearly related to $\log m$, as the x-axis is on a logarithmic scale. This indicates that our estimate is accurate. Additionally, we can see in the case that m is not sufficiently large, e.g. m = 1000, our estimation fits well, too. The details of the experiment is provided in Appendix D.

4.3 Secondary plateau stage

4.3.1 Long-term plateau

We now focus on the dynamics behavior at the secondary plateau stage and show that the dynamics can be approximately viewed as Eq. (21) due to the stability of the dynamics near critical point. Also, we consider the case $\frac{1}{2} < \alpha \le \frac{3}{2}$ and another case is similar. First, we recall for sufficiently large m and small δ' , the following inequalities hold at $t = T_{\rm d}$ by Theorem 2:

(i).
$$|K - 1| \le \delta$$
 and $|K' - 2| \le \delta$.

(ii).
$$q_{\max} \leq \frac{1}{m^{\frac{1}{2} - (2\alpha - 1)\delta'}}$$
.

(iii).
$$\max_{k \in m, i \in [2:d]} |w_k^i| \le \frac{1}{m^{\alpha - 2(2\alpha - 1)\delta'}}$$

(iv).
$$\left(\sum_{k=1}^{m} (w_k^i)^2\right)^{\frac{1}{2}} \le C \min \left\{ \frac{1}{m^{\frac{2\alpha-1}{2}}}, \frac{\log m}{m^{1-5(2\alpha-1)\delta'}} \right\}$$

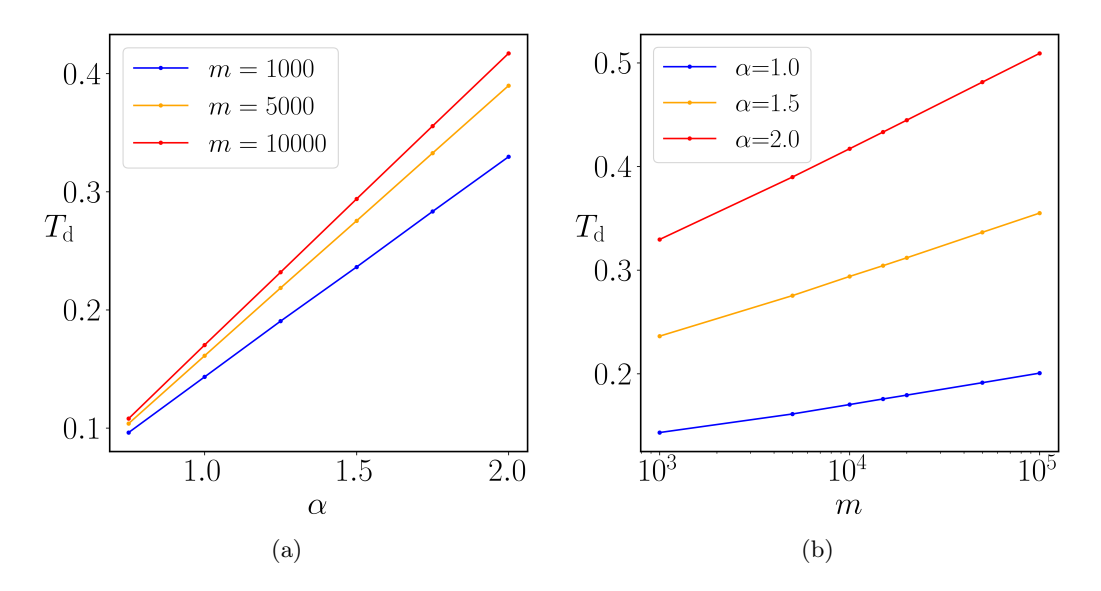


Figure 2: Descent time T_d with respect to $\alpha(a)$ and m(b)

Based on above estimation, we will give a description of the secondary plateau stage. Define $T_3 = \sup\{t \mid q_{\max} \leq \frac{1}{m^{\alpha_3}}\}$ where $\alpha_3 < \frac{1}{2} - \alpha_2$ and $T_4 = \sup\{t \mid 1 \leq K' \leq 3\}$, where C > 1. Here we take $\alpha_3 = 0.4$ since δ' can be sufficiently small if m is large. It should be noted that taking $\alpha_3 = 0.4$ is just to show that neural network will stay near the "critical point" for a long time. We also define

$$T_{\rm sp} = T_{\rm d} + \frac{1}{40} \frac{1}{\beta} \log m \tag{63}$$

as the end of the secondary plateau stage. It means that the secondary plateau will last for a considerable amount of time.

Theorem 3 (Long secondary plateau). For $\delta \in (0,1)$, sufficiently large m and given α , with probability at least $1-\delta$ over the choice of $\boldsymbol{\theta}$, the secondary plateau will longer than the first two stages significantly. That is

$$\frac{T_{\rm sp} - T_{\rm d}}{T_{\rm d}} \gg 1. \tag{64}$$

Moreover, loss will will stagnate for an extended period on the secondary plateau. That is

$$\frac{|R(\boldsymbol{\theta}(T_{\rm sp})) - R(\boldsymbol{\theta}(T_{\rm d}))|}{|R(\boldsymbol{\theta}(T_{\rm d}) - R(\boldsymbol{\theta}(T_{\rm p}))|} \frac{T_{\rm d} - T_{\rm p}}{T_{\rm sp} - T_{\rm d}} \approx 0.$$
(65)

The overall proof is similar to the previous one. Based on growth Lemma 2, we have following proposition.

Proposition 7 (Estimate of weights in non-condensed directions at secondary plateau stage). For $\delta \in (0,1)$ and sufficiently large m, with probability at least $1-\delta$ over the choice of $\boldsymbol{\theta}$, for $T_{\rm d} \leq t \leq \min\{T_3, T_4, T_{\rm sp}\}$ and $i=2,\ldots,d, \sum_{k=1}^m (w_k^i)^2$ will be controlled by following inequality,

$$\left(\sum_{k=1}^{m} \left(w_k^i(t)\right)^2\right)^{\frac{1}{2}} \le C \max\left\{\frac{1}{m^{\frac{2\alpha-1}{2}}}, \frac{\log m}{m^{1-5(2\alpha-1)\delta'}}\right\} + C\frac{(\log m)^2}{m^{5\alpha_3 - \frac{3}{2}}}.$$
(66)

Proof. By growth Lemma 2, we get for sufficiently large m

$$\left(\sum_{k=1}^{m} \left(w_{k}^{i}(t)\right)^{2}\right)^{\frac{1}{2}} \leq \left(\sum_{k=1}^{m} \left(w_{k}^{i}(T_{d})\right)^{2}\right)^{\frac{1}{2}} \\
\leq C \max\left\{\frac{1}{m^{\frac{2\alpha-1}{2}}}, \frac{\log m}{m^{1-5(2\alpha-1)\delta'}}\right\} + C\frac{1}{\beta} \frac{\log m}{m^{5\alpha_{3}-\frac{3}{2}}} \\
\leq C \max\left\{\frac{1}{m^{\frac{2\alpha-1}{2}}}, \frac{\log m}{m^{1-5(2\alpha-1)\delta'}}\right\} + C\frac{(\log m)^{2}}{m^{5\alpha_{3}-\frac{3}{2}}}.$$

Now we turn to the proof of Theorem 3.

Proof of Theorem 3. By definition of $T_{\rm sp}$, inequality (64) is straightforward. Therefore, what actually needs to be proven is that the loss is indeed at the secondary plateau at time $T_{\rm sp}$, which corresponds to inequality (65). With the help of T_3 , this only requires proving

$$T_{\rm sp} \le T_3. \tag{67}$$

The remaining part only requires simple calculations. The whole proof can be divided into three parts.

(i). We first establish a control of w_k^i where $i \in [2:d]$ at $t = \min\{T_3, T_4, T_{\rm sp}\}$. That is

$$\begin{split} |w_k^i(t)| & \leq |w_k^i(T_{\rm d})| + \int_{T_{\rm d}}^t |a_k| \sum_{k=1}^m |a_k| |w_k^i| {\rm d}s + \int_{T_{\rm d}}^t |g_k^i| {\rm d}s \\ & \leq \frac{1}{m^{\alpha - 2(2\alpha - 1)\delta'}} + \int_{T_{\rm d}}^t \frac{1}{m^{\alpha_3}} C \max\left\{\frac{1}{m^{\frac{2\alpha - 1}{2}}}, \frac{\log m}{m^{1 - 5(2\alpha - 1)\delta'}}\right\} {\rm d}s \\ & + \int_{T_{\rm d}}^t C \frac{\log m}{m^{5\alpha_3 - \frac{3}{2}}} {\rm d}s. \end{split}$$

As a result, $|w_k^i| < \frac{1}{m^{\alpha_3}}$ at $t = \min\{T_3, T_4, \frac{1}{40}\frac{1}{\beta}\log m\}$, given that $\alpha_3 = 0.4$ and β is a given small constant, which allows us to choose m to be sufficiently large. This implies that q_{\max} can't be attained by w_k^i .

(ii). Next, we examine the dynamics of K:

$$\frac{\mathrm{d}K}{\mathrm{d}t} = K'(1-K) - \sum_{i=2}^{d} \left(\sum_{k=1}^{m} a_k w_k^i \right) \left(\sum_{k=1}^{m} w_k^1 w_k^i \right) + \sum_{k=1}^{m} w_k^1 f_k + \sum_{k=1}^{m} a_k g_k^1.$$

Then for $t \leq \min\{T_3, T_4, T_{\rm sp}\}$, we have

$$(K-1)^2(t) - (K-1)^2(T_d) \le C\varepsilon \int_{T_d}^t |K-1| ds.$$

where $\varepsilon = \min\left\{\frac{1}{m^{2\alpha-1}}, \frac{(\log m)^2}{m^{2-10(2\alpha-1)\delta'}}, \frac{1}{m^{5\alpha_3-\frac{3}{2}}}\right\}$. By applying the Gronwall inequality, we find that the following inequality holds for sufficiently large m,

$$|K - 1|(t) \le \beta + C\varepsilon \frac{1}{\beta} \log m \le 2\beta.$$
 (68)

(iii). We assert that min $\{T_3, T_4\} \ge \frac{1}{40} \frac{1}{\beta} \log m$. If this is not the case, there are two possible cases:

- $T_3 \leq \frac{1}{40} \frac{1}{\beta} \log m \text{ and } T_3 \leq T_4.$
- $T_4 \leq \frac{1}{40} \frac{1}{\beta} \log m \text{ and } T_4 \leq T_4.$

We will proceed with a case-by-case analysis. If case 1 holds, the main technique we use is the conservation law. Since

$$4K\frac{dK}{dt} - K'\frac{dK'}{dt} = -4K\sum_{i=2}^{d} \left(\sum_{k=1}^{m} a_k w_k^i\right) \left(\sum_{k=1}^{m} w_k^1 w_k^i\right) + 2K'\sum_{i=2}^{d} \left(\sum_{k=1}^{m} a_k w_k^i\right)^2 - 4K\left(\sum_{k=1}^{m} w_k^1 f_k + \sum_{k=1}^{m} a_k g_k\right) + K'\left(\sum_{k=1}^{m} a_k f_k + \sum_{k=1}^{m} w_k^1 g_k\right).$$

The right hand of the equality is less than $C\varepsilon(K')^2$. Similar to the proof of Proposition 6, $K/K'\approx\frac{1}{2}$, which means $K'\approx 2$ since $|K-1|\leq 2\beta$. It contradicts with the definition of T_3 .

If case 2 holds, the technique we now use is the point estimation which is similar to what we have done before but with some difference.

$$\frac{\mathrm{d}a_k}{\mathrm{d}t} = w_k^1 - \left(\sum_{l=1}^m a_l w_l^1\right) w_k^1 - \sum_{i=2}^d \left(\sum_{l=1}^m a_l w_l^i\right) w_k^i + f_k,$$

$$\frac{\mathrm{d}w_k^1}{\mathrm{d}t} = a_k - \left(\sum_{l=1}^m a_l w_l^1\right) a_k + g_k^1.$$

Then for $t \leq T_4$,

$$|a_{k}(t)| \leq |a_{k}(T_{p})| + 2\beta \int_{T_{p}}^{t} |w_{k}^{1}| ds + \int_{T_{p}}^{t} C \min\{\frac{1}{m^{\frac{2\alpha-1}{2}}}, \frac{1}{m^{1-5c_{0}}}\} \frac{1}{m^{\alpha-c_{0}}} ds,$$

$$|w_{k}^{1}(t)| \leq |w_{k}^{1}(T_{p})| + 2\beta \int_{T_{p}}^{t} |a_{k}| ds + \int_{T_{p}}^{t} \frac{1}{m^{\frac{3}{2}-5c_{0}}} ds.$$

$$(69)$$

It means that

$$v(t) \le (1 + e^{2\beta(t - T_p)})v(t_0).$$
 (70)

Taking $t - T_p = \frac{1}{40} \frac{1}{\beta} \log m$, we find that $q_{\text{max}} \leq \frac{1}{m^{0.45}}$. It leads to a contradiction.

As a result, $\min\{T_4, T_\beta\} \leq \frac{1}{40} \frac{1}{\beta} \log m$. Moreover, we have $T_4 \leq T_3$ by similar discussion.

4.3.2Plateau departure

Next question is how do the dynamics drive the parameters away from the critical point? Here, we give some insights by experiments and heuristic analysis. Recall the definition of f_k and g_k .

$$f_{k} = \int_{\mathbb{R}^{d}} f(\boldsymbol{x}) \left(\frac{1}{3!} \sigma^{(3)}(\xi_{k}(\boldsymbol{x})) (\boldsymbol{w}_{k}^{\top} \boldsymbol{x})^{3} \right) \rho(\boldsymbol{x}) \, d\boldsymbol{x}$$

$$- \int_{\mathbb{R}^{d}} \left(\sum_{l=1}^{m} \frac{1}{3!} \sigma^{(3)}(\xi_{l}(\boldsymbol{x})) a_{l}(\boldsymbol{w}_{l}^{\top} \boldsymbol{x})^{3} \right) (\boldsymbol{w}_{k}^{\top} \boldsymbol{x}) \rho(\boldsymbol{x}) \, d\boldsymbol{x}$$

$$- \int_{\mathbb{R}^{d}} \left(\sum_{l=1}^{m} a_{l} \left(\boldsymbol{w}_{l}^{\top} \boldsymbol{x} + \frac{1}{3!} \sigma^{(3)}(\xi_{l}(\boldsymbol{x})) (\boldsymbol{w}_{l}^{\top} \boldsymbol{x})^{3} \right) \right) \left(\frac{1}{3!} \sigma^{(3)}(\xi_{k}(\boldsymbol{x})) (\boldsymbol{w}_{k}^{\top} \boldsymbol{x})^{3} \right) \rho(\boldsymbol{x}) \, d\boldsymbol{x}.$$

$$\boldsymbol{g}_{k} = \int_{\mathbb{R}^{d}} f(\boldsymbol{x}) a_{k} \left(\frac{1}{2!} \sigma^{(3)} \left(\eta_{k}(\boldsymbol{x}) \right) \left(\boldsymbol{w}_{k}^{\top} \boldsymbol{x} \right)^{2} \right) \boldsymbol{x} \rho(\boldsymbol{x}) \, d\boldsymbol{x}$$

$$- \int_{\mathbb{R}^{d}} \left(\sum_{l=1}^{m} a_{l} \left(\boldsymbol{w}_{l}^{\top} \boldsymbol{x} \right) \right) a_{k} \left(\frac{1}{2!} \sigma^{(3)} \left(\eta_{k}(\boldsymbol{x}) \right) \left(\boldsymbol{w}_{k}^{\top} \boldsymbol{x} \right)^{2} \right) \boldsymbol{x} \rho(\boldsymbol{x}) \, d\boldsymbol{x}$$

$$- \int_{\mathbb{R}^{d}} \left(\sum_{l=1}^{m} a_{l} \frac{1}{3!} \sigma^{(3)} \left(\xi_{l}(\boldsymbol{x}) \right) \left(\boldsymbol{w}_{l}^{\top} \boldsymbol{x} \right)^{3} \right) a_{k} \left(1 + \frac{1}{2!} \sigma^{(3)} \left(\eta_{k}(\boldsymbol{x}) \right) \left(\boldsymbol{w}_{k}^{\top} \boldsymbol{x} \right)^{2} \right) \boldsymbol{x} \rho(\boldsymbol{x}) \, d\boldsymbol{x}.$$

In above discussion, we actually use linear model $\sum_{k=1}^{m} a_k \mathbf{w}_k^{\top} \mathbf{x}$ to characterize the behavior of the nonlinear model f_{θ} . On the secondary plateau, the model's nonlinearity gradually begins to emerge. The first noticeable effect is that, at this stage, the roles of a and w are no longer equivalent. For simplicity, we consider a 1-d example for illustration and truncate only up to the third order, as we are considering the tanh activation function. As a result, f_k and g_k will be approximated by

$$f_k = -\frac{1}{3!}c_4\sigma^{(3)}(0)\left(\sum_{l=1}^m a_l w_l^3\right)w_k + \frac{1}{3!}b_3\sigma^{(3)}(0)w_k^3,$$

$$\mathbf{g}_k = -\frac{1}{3!}c_4\sigma^{(3)}(0)\left(\sum_{l=1}^m a_l w_l^3\right)a_k + \frac{1}{2!}b_3\sigma^{(3)}(0)a_k w_k^2$$

$$-\frac{1}{2!}\sigma^{(3)}(0)c_4\left(\sum_{l=1}^m a_l w_l\right)a_k w_k^2,$$

where $c_4 = \int x^4 \rho(x) dx$ and $b_3 = \int f(x) x^3 \rho(x) dx$. Substituting the condition of critical point $\sum_{k=1}^m a_k w_k = 1$ into whole dynamics, we obtain $\frac{d(\sum_{k=1}^m a_k^2)}{d(\sum_{k=1}^m w_k^2)} \neq 1$. Thus, the roles of \boldsymbol{a} and \boldsymbol{w} begin to shift. Once this shift progresses sufficiently, the model's

nonlinearity truly starts to manifest, and the loss moves away from the secondary plateau.

4.3.3 Experiment

We have characterized the microscopic behavior of the model parameters across the three stages in the previous proofs and discussions. The distribution of input weights a and the output weights w gradually become consistent during the descent stage. At this time the training goes into the secondary plateau, it is after the weights distributions diverge that the descent of training loss begins once again. At the meantime, the norms of weights exceed the linear regime and enter the nonlinear region. To experimentally demonstrate that this dynamical phenomenon exists universally under our assumptions, we test different target functions and display the ratio of their weights norms, along with the relative Wasserstein distance between the weights distributions in Fig. 3. We can observe in Fig. 3(a) that this ratio stays around the value of 1 (gold dash line) for a period before the time it begins to change, after which the behavior of weights depends on the settings of different target functions. Moreover, the relative Wassertein distances in Fig. 3 approach zero synchronously, indicating that the input weights and output weight have the same distribution as well as the same norm at this time. From Fig. 3 we can obtain a consistent performance of the first three stages for different target functions, validating the correctness of our theorems. Additionally, the details of the setting are provided in the Appendix D.

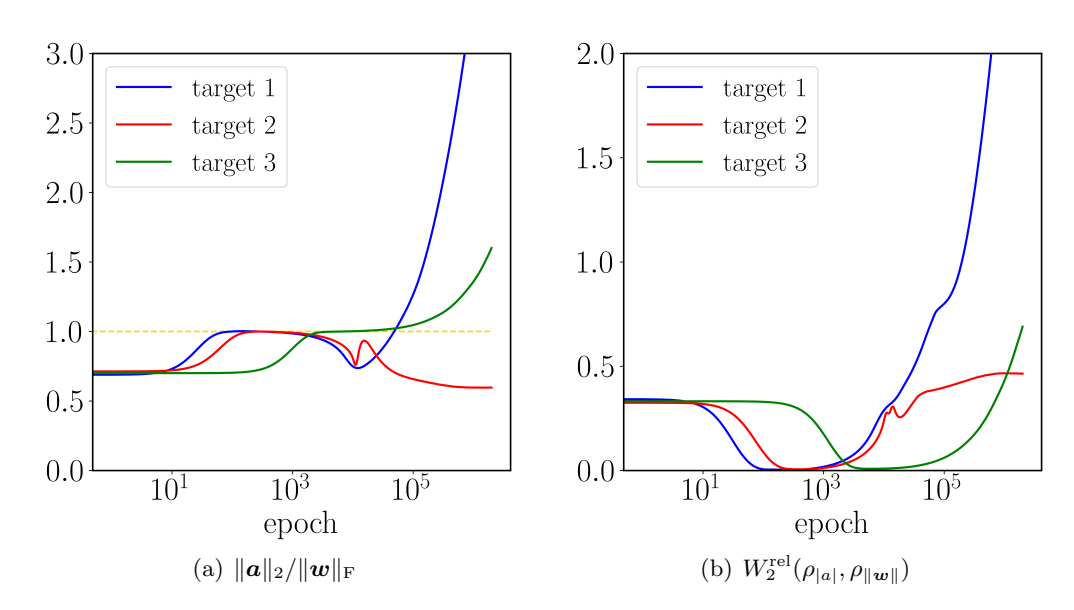


Figure 3: Panel (a) and (b): Towards different target function, the curve of ratio of weight norms and relative Wasserstein distance, respectively.

5 Summary

In this paper, we consider the dynamics of two-layer neural networks during training with small initialization. We divide the initial training stages into three distinct stages and provide a rigorous theoretical description for each stage in an over-parameterized setting. Additionally, we introduce Wasserstein metric to characterize the distribution of weights during training. Our conclusions further extend previous studies on the training process with small initialization. Through our research, we deepen the understanding of the training dynamics of neural networks, not only from the macroscopic perspective of loss performance but also from the more microscopic perspective of parameter behavior.

6 Acknowledgments

This work is sponsored by the National Key R&D Program of China Grant No. 2022YFA1008200 (T. L.), the National Natural Science Foundation of China Grant No. 12101401 (T. L.), Shanghai Municipal Science and Technology Key Project No. 22JC1401500 (T. L.), Shanghai Municipal of Science and Technology Major Project No. 2021SHZDZX0102 (T. L.).

A Notation List

Notation	Description	Notation	Description
m, α	width and hyperparameter in initialization	T_1, T_2, T_3, T_4	milestones for characterizing the stages, see Eqs. (26) and (48) and Section 4.3.1
K,K'	macroscopic measurement of parameters, see Eq. (17)	$T_{ m test}$	intuitive conjecture milestone, see Lemma 2
$q_{ m max}, ilde{q}_{ m max}$	neuron-wise L_{∞} norm, see Eqs. (11) and (24)	$T_{ m p}$	milestone for the initial plateau stage, see Theorem 1
$r_{ m max}$	weights deviation from linearized flow, see Eq. (25)	$T_{ m d}$	milestone for the initial descent stage, see Eq. (44)
$W_2(\rho_1,\rho_2)$	Wasserstein distance between ρ_1 and ρ_2 , see Eq. (13)	$T_{ m sp}$	milestone for the secondary plateau stage, see Eq. (63)

Table 2: Table of notation list

B Derivation of Main Dynamics

In this section, we present the explicit derivation of Eq. (8). Since we are considering gradient descent, the dynamics of parameters will obey

$$\frac{\mathrm{d}a_k}{\mathrm{d}t} = -\frac{\partial R}{\partial a_k},$$
$$\frac{\mathrm{d}\boldsymbol{w}_k}{\mathrm{d}t} = -\frac{\partial R}{\partial \boldsymbol{w}_k}.$$

We separately compute the equations for a_k and w_k as follows. For a_k , we have

$$\frac{\mathrm{d}a_k}{\mathrm{d}t} = -\int_{\mathbb{R}^d} \left(f_{\boldsymbol{\theta}}(\boldsymbol{x}) - f(\boldsymbol{x}) \right) \sigma(\boldsymbol{w}_k^{\top} \boldsymbol{x}) \rho(\boldsymbol{x}) \, \mathrm{d}\boldsymbol{x}$$
$$= -\int_{\mathbb{R}^d} \left(\sum_{k=1}^m a_k \sigma(\boldsymbol{w}_k^{\top} \boldsymbol{x}) - f(\boldsymbol{x}) \right) \sigma(\boldsymbol{w}_k^{\top} \boldsymbol{x}) \rho(\boldsymbol{x}) \, \mathrm{d}\boldsymbol{x}.$$

By taylor expansion and Assumption 3, we have

$$\frac{\mathrm{d}a_k}{\mathrm{d}t} = -\int_{\mathbb{R}^d} \left(\sum_{l=1}^m a_l \left(\boldsymbol{w}_l^\top \boldsymbol{x} + \frac{1}{3!} \sigma^{(3)}(\xi_l(\boldsymbol{x})) (\boldsymbol{w}_l^\top \boldsymbol{x})^3 \right) - f(\boldsymbol{x}) \right) \left(\boldsymbol{w}_k^\top \boldsymbol{x} + \frac{1}{3!} \sigma^{(3)}(\xi_k(\boldsymbol{x})) (\boldsymbol{w}_k^\top \boldsymbol{x})^3 \right) \rho(\boldsymbol{x}) \, \mathrm{d}\boldsymbol{x}$$

After expanding and regrouping the terms, we can rewrite the above expression in a more streamlined form.

$$\frac{\mathrm{d}a_{k}}{\mathrm{d}t} = \int_{\mathbb{R}^{d}} f(\boldsymbol{x})(\boldsymbol{w}_{k}^{\top}\boldsymbol{x})\rho(\boldsymbol{x})\,\mathrm{d}\boldsymbol{x} - \int_{\mathbb{R}^{d}} \left(\sum_{l=1}^{m} a_{l}\boldsymbol{w}_{l}^{\top}\boldsymbol{x}\right)(\boldsymbol{w}_{k}^{\top}\boldsymbol{x})\rho(\boldsymbol{x})\,\mathrm{d}\boldsymbol{x} \\
+ \int_{\mathbb{R}^{d}} f(\boldsymbol{x})\left(\frac{1}{3!}\sigma^{(3)}(\xi_{k}(\boldsymbol{x}))(\boldsymbol{w}_{k}^{\top}\boldsymbol{x})^{3}\right)\rho(\boldsymbol{x})\,\mathrm{d}\boldsymbol{x} \\
- \int_{\mathbb{R}^{d}} \left(\sum_{l=1}^{m} \frac{1}{3!}\sigma^{(3)}(\xi_{l}(\boldsymbol{x}))a_{l}(\boldsymbol{w}_{l}^{\top}\boldsymbol{x})^{3}\right)(\boldsymbol{w}_{k}^{\top}\boldsymbol{x})\rho(\boldsymbol{x})\,\mathrm{d}\boldsymbol{x} \\
- \int_{\mathbb{R}^{d}} \left(\sum_{l=1}^{m} a_{l}\left(\boldsymbol{w}_{l}^{\top}\boldsymbol{x} + \frac{1}{3!}\sigma^{(3)}(\xi_{l}(\boldsymbol{x}))(\boldsymbol{w}_{l}^{\top}\boldsymbol{x})^{3}\right)\right)\left(\frac{1}{3!}\sigma^{(3)}(\xi_{k}(\boldsymbol{x}))(\boldsymbol{w}_{k}^{\top}\boldsymbol{x})^{3}\right)\rho(\boldsymbol{x})\,\mathrm{d}\boldsymbol{x}. \tag{71}$$

Based on Assumption 2, we have

$$\int_{\mathbb{R}^d} f(\boldsymbol{x})(\boldsymbol{w}_k^{\top} \boldsymbol{x}) \rho(\boldsymbol{x}) \, \mathrm{d}\boldsymbol{x} = w_k^1.$$
 (72)

Using Assumption 1, we have

$$\int_{\mathbb{R}^{d}} \left(\sum_{l=1}^{m} a_{l} \boldsymbol{w}_{l}^{\top} \boldsymbol{x} \right) (\boldsymbol{w}_{k}^{\top} \boldsymbol{x}) \rho(\boldsymbol{x}) \, d\boldsymbol{x} = \int_{\mathbb{R}^{d}} \left(\sum_{l=1}^{m} a_{l} \left(\sum_{i=1}^{d} w_{l}^{i} x_{i} \right) \right) \left(\sum_{j=1}^{d} w_{k}^{j} x_{j} \right) \rho(\boldsymbol{x}) \, d\boldsymbol{x} \\
= \int_{\mathbb{R}^{d}} \left(\sum_{i=1}^{d} \left(\sum_{l=1}^{m} a_{l} w_{l}^{i} \right) x_{i} \right) \left(\sum_{j=1}^{d} w_{k}^{j} x_{j} \right) \rho(\boldsymbol{x}) \, d\boldsymbol{x} \qquad (73)$$

$$= \sum_{i=1}^{d} \left(\sum_{l=1}^{m} a_{l} w_{l}^{i} \right) w_{k}^{i}.$$

Combining Eqs. (71), (72), (73) with the definition of f_k , we have

$$\frac{\mathrm{d}a_k}{\mathrm{d}t} = w_k^1 - \sum_{i=1}^d \left(\sum_{l=1}^m a_l w_l^i\right) w_k^i + f_k.$$

For \boldsymbol{w}_k , we have

$$\frac{\mathrm{d}\boldsymbol{w}_k}{\mathrm{d}t} = -\int_{\mathbb{R}^d} \left(f_{\boldsymbol{\theta}}(\boldsymbol{x}) - f(\boldsymbol{x}) \right) a_k \sigma^{(1)}(\boldsymbol{w}_k^{\top} \boldsymbol{x}) \boldsymbol{x} \rho(\boldsymbol{x}) \, \mathrm{d}\boldsymbol{x}$$

$$= -\int_{\mathbb{R}^d} \left(\sum_{l=1}^m a_l \sigma(\boldsymbol{w}_l^{\top} \boldsymbol{x}) - f(\boldsymbol{x}) \right) a_k \sigma^{(1)}(\boldsymbol{w}_k^{\top} \boldsymbol{x}) \boldsymbol{x} \rho(\boldsymbol{x}) \, \mathrm{d}\boldsymbol{x}$$

By Taylor expansion and Assumption 3, we have

$$\frac{\mathrm{d}\boldsymbol{w}_k}{\mathrm{d}t} = -\int_{\mathbb{R}^d} \left(\sum_{l=1}^m a_l \left(\boldsymbol{w}_l^\top \boldsymbol{x} + \frac{1}{3!} \sigma^{(3)}(\xi_l(\boldsymbol{x})) (\boldsymbol{w}_l^\top \boldsymbol{x})^3 \right) - f(\boldsymbol{x}) \right) a_k \left(1 + \frac{1}{2!} \sigma^{(3)}(\eta_k(\boldsymbol{x})) (\boldsymbol{w}_k^\top \boldsymbol{x})^2 \right) \boldsymbol{x} \rho(\boldsymbol{x}) \, \mathrm{d}\boldsymbol{x}$$

Similarly, by an appropriate reformulation, the above expression can be written in a more concise form.

$$\frac{\mathrm{d}\boldsymbol{w}}{\mathrm{d}t} = -\int_{\mathbb{R}^d} \left(\sum_{l=1}^m a_l(\boldsymbol{w}_l^\top \boldsymbol{x}) - f(\boldsymbol{x}) \right) a_k \boldsymbol{x} \rho(\boldsymbol{x}) \, \mathrm{d}\boldsymbol{x}
+ \int_{\mathbb{R}^d} f(\boldsymbol{x}) a_k \left(\frac{1}{2!} \sigma^{(3)} \left(\eta_k(\boldsymbol{x}) \right) \left(\boldsymbol{w}_k^\top \boldsymbol{x} \right)^2 \right) \boldsymbol{x} \rho(\boldsymbol{x}) \, \mathrm{d}\boldsymbol{x}
- \int_{\mathbb{R}^d} \left(\sum_{l=1}^m a_l \left(\boldsymbol{w}_l^\top \boldsymbol{x} \right) \right) a_k \left(\frac{1}{2!} \sigma^{(3)} \left(\eta_k(\boldsymbol{x}) \right) \left(\boldsymbol{w}_k^\top \boldsymbol{x} \right)^2 \right) \boldsymbol{x} \rho(\boldsymbol{x}) \, \mathrm{d}\boldsymbol{x}
- \int_{\mathbb{R}^d} \left(\sum_{l=1}^m a_l \frac{1}{3!} \sigma^{(3)} \left(\xi_l(\boldsymbol{x}) \right) \left(\boldsymbol{w}_l^\top \boldsymbol{x} \right)^3 \right) a_k \left(1 + \frac{1}{2!} \sigma^{(3)} \left(\eta_k(\boldsymbol{x}) \right) \left(\boldsymbol{w}_k^\top \boldsymbol{x} \right)^2 \right) \boldsymbol{x} \rho(\boldsymbol{x}) \, \mathrm{d}\boldsymbol{x}.$$

Based on the definition of g_k , we have Eq. (8). Similar to the derivation of a_k , by Assumptions 1 and 2, we can reformulation above equation into a entry-wise form which corresponds to Eq. (10).

C Several Estimates on the Initialization

We begin this part by an estimate on standard Gaussian vectors.

Lemma 3 (Bounds on initial parameters; rephrased from Lemma 1 [2]). Given any $\delta \in (0,1)$, we have with probability at least $1 - \delta$ over the choice of $\boldsymbol{\theta}$,

$$\max_{k \in [m]} \{ |a_k(0)|, \|\boldsymbol{w}_k(0)\|_{\infty} \} \le \frac{1}{m^{\alpha}} \sqrt{2 \log \frac{2m(d+1)}{\delta}}.$$
 (74)

Proof. If $X = \mathcal{N}(0,1)$, then for any $\eta > 0$,

$$\mathbb{P}(|X| > \eta) \le 2 \exp\left(-\frac{1}{2}\eta^2\right).$$

Since for $k \in [m]$,

$$a_k = \mathcal{N}(0, \frac{1}{m^{2\alpha}}), \quad \boldsymbol{w}_k^0 = \mathcal{N}\left(\boldsymbol{0}, \frac{1}{m^{2\alpha}}\boldsymbol{I}_d\right),$$

where

$$\boldsymbol{w}_k := \left[w_k^1, w_k^2, \cdots, w_k^d \right]^{ op},$$

then for any $k \in [m]$ and $j \in [d]$,

$$m^{\alpha} a_k = \mathcal{N}(0, 1),$$

$$m^{\alpha} w_k^j = \mathcal{N}(0, 1),$$

and they are all independent with each other. As we set

$$\eta = \sqrt{2\log\frac{2m(d+1)}{\delta}},$$

we obtain that

$$\begin{split} & \mathbb{P}\left(\max_{k \in [m]} \left\{ \left| m^{\alpha} a_{k} \right|, \left\| m^{\alpha} \boldsymbol{w}_{k} \right\|_{\infty} \right\} > \eta \right) \\ & = \mathbb{P}\left(\max_{k \in [m], j \in [d]} \left\{ \left| m^{\alpha} a_{k} \right|, \left| m^{\alpha} w_{k}^{j} \right| \right\} > \eta \right) \\ & = \mathbb{P}\left(\bigcup_{k=1}^{m} \left[\left(\left| m^{\alpha} a_{k} \right| > \eta \right) \bigcup \left(\bigcup_{j=1}^{d} \left(\left| m^{\alpha} w_{k}^{j} \right| > \eta \right) \right) \right] \right) \\ & \leq \sum_{k=1}^{m} \mathbb{P}\left(\left| m^{\alpha} a_{k} \right| > \eta \right) + \sum_{k=1}^{m} \sum_{j=1}^{d} \mathbb{P}\left(\left| m^{\alpha} w_{k}^{j} \right| > \eta \right) \\ & \leq 2m \exp\left(-\frac{1}{2} \eta^{2} \right) + 2md \exp\left(-\frac{1}{2} \eta^{2} \right) \\ & = 2m(d+1) \exp\left(-\frac{1}{2} \eta^{2} \right) = \delta. \end{split}$$

Next we would like to introduce the sub-exponential norm [23] of a random variable and Bernstein's Inequality.

Definition 1 (Sub-exponential norm). The sub-exponential norm of a random variable X is defined as

$$\|X\|_{\psi_1} := \inf \left\{ s > 0 \mid \mathbb{E}_X \left[e^{[X|/s]} \right] \le 2 \right\}.$$
 (75)

In particular, we denote the sub-exponential norm of a $\chi^2(d)$ random variable X by $C_{\psi,d} := \|X\|_{\psi_1}$. Here the χ^2 distribution with d degrees of freedom has the probability density function

$$f_{\rm X}(z) = \frac{1}{2^{d/2}\Gamma(d/2)} z^{d/2-1} e^{-z/2}$$

Remark 9. Note that

$$\mathbb{E}_{\mathbf{X} \sim \chi^2(d)} \mathbf{e}^{|\mathbf{X}|/2} = \int_0^{+\infty} \frac{1}{2^{d/2} \Gamma(d/2)} z^{d/2 - 1} \, dz = +\infty,$$

$$\lim_{s \to +\infty} \mathbb{E}_{\mathbf{X} \sim \chi^2(d)} \mathbf{e}^{|\mathbf{X}|/s} = \lim_{s \to +\infty} \int_0^{+\infty} \frac{1}{2^{d/2} \Gamma(d/2)} z^{d/2 - 1} \mathbf{e}^{-z/2 + z/s} \, dz = 1 < 2.$$

These imply that $2 \leq C_{\psi,d} < +\infty$.

Theorem 4 (Bernstein's inequality). Let $\{X_k\}_{k=1}^m$ be i.i.d. sub-exponential random variables satisfying

$$\mathbb{E}X_1=\mu$$
,

then for any $\eta \geq 0$, we have

$$\mathbb{P}\left(\left|\frac{1}{m}\sum_{k=1}^{m}\mathbf{X}_{k}-\mu\right|\geq\eta\right)\leq2\exp\left(-C_{0}m\min\left(\frac{\eta^{2}}{\left\|\mathbf{X}_{1}\right\|_{\psi_{1}}^{2}},\frac{\eta}{\left\|\mathbf{X}_{1}\right\|_{\psi_{1}}}\right)\right)$$

for some absolute constant C_0 .

Proposition 8 (Upper and lower bounds of initial parameters; rephrased from Proposition 1 [2]). Given any $\delta \in (0,1)$, if

$$m = \Omega\left(\log\frac{4}{\delta}\right),\,$$

then with probability at least $1 - \delta$ over the choice of θ , and

$$\begin{split} \sqrt{\frac{(d+1)}{2}\frac{1}{m^{2\alpha-1}}} &\leq \|\boldsymbol{\theta}\|_2 \leq \sqrt{\frac{3(d+1)}{2}\frac{1}{m^{2\alpha-1}}}, \\ \sqrt{\frac{1}{2}\frac{1}{m^{2\alpha-1}}} &\leq \|\boldsymbol{a}\|_2 \leq \sqrt{\frac{3}{2}\frac{1}{m^{2\alpha-1}}}, \\ \sqrt{\frac{d}{2}\frac{1}{m^{2\alpha-1}}} &\leq \|\boldsymbol{w}\|_{\mathrm{F}} \leq \sqrt{\frac{3d}{2}\frac{1}{m^{2\alpha-1}}}. \end{split}$$

Proof. Since

$$(m^{\alpha}a_1)^2, (m^{\alpha}a_2)^2, \cdots, (m^{\alpha}a_m)^2 \sim \chi^2(1)$$

are i.i.d. sub-exponential random variables with

$$\mathbb{E}\left(m^{\alpha}a_1\right)^2 = 1.$$

By application of Theorem 3, we have

$$\mathbb{P}\left(\left|\frac{1}{m}\sum_{k=1}^{m}(m^{\alpha}a_{k})^{2}-1\right|\geq\eta\right)\leq2\exp\left(-C_{0}m\min\left(\frac{\eta^{2}}{C_{\psi,1}^{2}},\frac{\eta}{C_{\psi,1}}\right)\right),$$

since $C_{\psi,1} \geq \frac{8}{3} > 2$, then for any $0 \leq \eta \leq 2$, it is obvious that

$$\min\left(\frac{\eta^2}{C_{\psi,1}^2}, \frac{\eta}{C_{\psi,1}}\right) = \frac{\eta^2}{C_{\psi,1}^2}.$$

We set

$$2\exp\left(-C_0m\frac{\eta^2}{C_{\psi,1}^2}\right) = \frac{\delta}{2},$$

and consequently,

$$\eta = \sqrt{\frac{C_{\psi,1}^2}{mC_0}} \log \frac{4}{\delta},$$

then with probability at least $1 - \frac{\delta}{2}$ over the choice of $\boldsymbol{\theta}$,

$$\frac{1}{m^{2\alpha-1}} \left(1 - \sqrt{\frac{C_{\psi,1}^2}{mC_0} \log \frac{4}{\delta}} \right) \le \|\boldsymbol{a}\|_2^2 \le \frac{1}{m^{2\alpha-1}} \left(1 + \sqrt{\frac{C_{\psi,1}^2}{mC_0} \log \frac{4}{\delta}} \right)$$

by choosing

$$m \ge \frac{4C_{\psi,1}^2}{C_0} \log \frac{4}{\delta}.$$

We obtain that

$$\sqrt{\frac{1}{m^{2\alpha-1}}\frac{1}{2}} \le \|\boldsymbol{a}\|_2 \le \sqrt{\frac{1}{m^{2\alpha-1}}\frac{3}{2}}.$$

The other inequalities are similar.

D Details of Experiment Settings

Considering the focus of this study is on the dynamical behavior in the training process of neural networks, it should be noted that we employ the gradient descent method with learning rate of 0.001 for simulating the gradient flow, this will be consistently applied throughout our paper. More detailed settings are as followings:

- m = [1000, 5000, 10000, 15000, 20000, 50000, 100000],
- $\alpha = [0.75, 1.0, 1.25, 1.5, 1.75, 2.0],$
- input data: $\{(x_i, f^*(x_i))\}_{i=1}^{n=1000}, \{x_i\}_i^n$ are equidistant points in [-15, 15],
- the target functions are $f_1^* = \tanh(x+7.5) + \tanh(x) + \tanh(x-7.5)$; $f_2^* = \tanh(x)$; $f_3^* = \sin(x)$.

In the experiment shown in Fig 1, we choose m = 5000, $\alpha = 1.0$ and target function f_1^* to exhibit the training dynamics; in Section 4.2.2, we use various choices of m and α as stated above to learn f_1^* , the result is shown in Fig 2; in Section 4.3.3, we fix $m = 5000, \alpha = 1.0$ and investigate the weights behavior for different target functions f_1^* , f_2^* , f_3^* , the result is shown in Fig 3.

References

- [1] Sanjeev Arora, Simon S Du, Wei Hu, Zhiyuan Li, Russ R Salakhutdinov, and Ruosong Wang, On exact computation with an infinitely wide neural net, Advances in Neural Information Processing Systems **32** (2019).
- [2] Zheng-An Chen, Yuqing Li, Tao Luo, Zhangchen Zhou, and Zhi-Qin John Xu, *Phase diagram of initial condensation for two-layer neural networks*, CSIAM Transactions on Applied Mathematics **5** (2024), no. 3, 448–514.
- [3] Zheng-An Chen and Tao Luo, On the dynamics of three-layer neural networks: initial condensation, arXiv preprint arXiv:2402.15958 (2024).
- [4] Lenaic Chizat and Francis Bach, On the global convergence of gradient descent for overparameterized models using optimal transport, Advances in Neural Information Processing Systems 31 (2018).
- [5] Alexey Dosovitskiy, An image is worth 16x16 words: Transformers for image recognition at scale, arXiv preprint arXiv:2010.11929 (2020).
- [6] Kenji Fukumizu and Shun-ichi Amari, Local minima and plateaus in hierarchical structures of multilayer perceptrons, Neural networks 13 (2000), no. 3, 317–327.
- [7] Jiaoyang Huang and Horng-Tzer Yau, Dynamics of deep neural networks and neural tangent hierarchy, International Conference on Machine Learning, PMLR, 2020, pp. 4542–4551.
- [8] Arthur Jacot, Franck Gabriel, and Clément Hongler, Neural tangent kernel: Convergence and generalization in neural networks, Advances in Neural Information Processing Systems 31 (2018).
- [9] Ziwei Ji and Matus Telgarsky, Directional convergence and alignment in deep learning, Advances in Neural Information Processing Systems 33 (2020), 17176–17186.

- [10] Akshay Kumar and Jarvis Haupt, Directional convergence near small initializations and saddles in two-homogeneous neural networks, Transactions on Machine Learning Research (2024).
- [11] Akshay Kumar and Jarvis Haupt, Early directional convergence in deep homogeneous neural networks for small initializations, arXiv preprint arXiv:2403.08121 (2024).
- [12] Tao Luo, Zhi-Qin John Xu, Zheng Ma, and Yaoyu Zhang, *Phase diagram for two-layer relu neural networks at infinite-width limit*, The Journal of Machine Learning Research **22** (2021), no. 1, 3327–3373.
- [13] Kaifeng Lyu and Jian Li, Gradient descent maximizes the margin of homogeneous neural networks, arXiv preprint arXiv:1906.05890 (2019).
- [14] Song Mei, Andrea Montanari, and Phan-Minh Nguyen, A mean field view of the landscape of two-layer neural networks, Proceedings of the National Academy of Sciences 115 (2018), no. 33, E7665–E7671.
- [15] Hancheng Min, Enrique Mallada, and Rene Vidal, Early neuron alignment in two-layer reluntation networks with small initialization, arXiv preprint arXiv:2307.12851 (2023).
- [16] Hyeyoung Park, S-I Amari, and Kenji Fukumizu, Adaptive natural gradient learning algorithms for various stochastic models, Neural Networks 13 (2000), no. 7, 755–764.
- [17] Pranav Rajpurkar, Jeremy Irvin, Robyn L Ball, Kaylie Zhu, Brandon Yang, Hershel Mehta, Tony Duan, Daisy Ding, Aarti Bagul, Curtis P Langlotz, et al., Deep learning for chest radiograph diagnosis: A retrospective comparison of the chexnext algorithm to practicing radiologists, PLoS medicine 15 (2018), no. 11, e1002686.
- [18] Grant Rotskoff and Eric Vanden-Eijnden, Parameters as interacting particles: long time convergence and asymptotic error scaling of neural networks, Advances in Neural Information Processing Systems 31 (2018).
- [19] David Saad and Sara A Solla, On-line learning in soft committee machines, Physical Review E 52 (1995), no. 4, 4225.
- [20] Omer Berat Sezer, Mehmet Ugur Gudelek, and Ahmet Murat Ozbayoglu, Financial time series forecasting with deep learning: A systematic literature review: 2005–2019, Applied soft computing 90 (2020), 106181.
- [21] Justin Sirignano and Konstantinos Spiliopoulos, Mean field analysis of neural networks: A central limit theorem, Stochastic Processes and their Applications 130 (2020), no. 3, 1820–1852.
- [22] A Vaswani, Attention is all you need, Advances in Neural Information Processing Systems (2017).
- [23] Roman Vershynin, Introduction to the non-asymptotic analysis of random matrices, arXiv preprint arXiv:1011.3027 (2010).
- [24] Tian Ye and Simon S Du, Global convergence of gradient descent for asymmetric low-rank matrix factorization, Advances in Neural Information Processing Systems **34** (2021), 1429–1439.

- [25] Hanxu Zhou, Zhou Qixuan, Tao Luo, Yaoyu Zhang, and Zhi-Qin Xu, Towards understanding the condensation of neural networks at initial training, Advances in Neural Information Processing Systems 35 (2022), 2184–2196.
- [26] Zhangchen Zhou, Hanxu Zhou, Yuqing Li, and Zhi-Qin John Xu, *Understanding the initial condensation of convolutional neural networks*, arXiv preprint arXiv:2305.09947 (2023).